Oceanic age and transient tracers: Analytical and numerical solutions

Carl Wunsch

Program in Atmospheres, Oceans and Climate, Department of Earth, Atmospheric and Planetary Sciences, Massachusetts Institute of Technology, Cambridge Massachusetts, USA

Received 12 January 2001; revised 16 August 2001; accepted 11 October 2001; published 12 June 2002.

[1] Transient tracers and the closely related "age" tracers exhibit a rich physical and mathematical structure even for problems of one space dimension. This richness tends to make interpretation of observations, which are inevitably thin in both space and time, difficult, in contrast to the situation in modeling studies. At least six different timescales and corresponding space scales can appear in one-dimensional problems. In higher dimensions the number of scales increases. Several examples of analytical and numerical solutions are explored for the light they cast on understanding a fluid flow. Boundary Green functions emerge as the fundamental physical/mathematical link between interior tracer distributions and surface and other boundary variations. With transient tracers in inverse calculations one should normally use the underlying tracer distributions to attempt to solve for fundamental fluid properties, such as the mixing coefficients, rather than ambiguous "ventilation" times, which among other problems, may be determined only by the detection threshold and are often mainly functions of the tracer decay constant rather than of fluid properties. Tracers that are transient only through stochastic boundary conditions show that large-scale space/time patterns can emerge in the tracer field, having little or no clear connection to the underlying fluid flow. *INDEX TERMS:* 4532 Oceanography: Physical: General circulation; 4568 Oceanography: Physical: Turbulence, diffusion, and mixing processes; 4203 Oceanography: General: Analytical modeling; 1635 Global Change: Oceans (4203); *KEYWORDS:* tracers, transient tracers, age tracers, advection/diffusion, mixing

1. Introduction

[2] Transient tracers have long been used in a variety of fields, including medicine, chemical engineering [*Nauman and Buffham*, 1983], meteorology [e.g., *Hall and Plumb*, 1994], and particularly, hydrology and related fields [e.g., *Lee*, 1999], as well as in physical oceanography; a simplified discussion of closely related problems in sedimentology is provided by *Boudreau* [1997]. In the oceanographic context, there exists a growing literature on comparisons of oceanic general circulation model (GCM) computations of transient tracers with observations [e.g., *England et al.*, 1994; *Duffy et al.*, 1995; *Craig et al.*, 1998; *Yamanaka et al.*, 1998] with varying claims to model skill in reproducing what is observed. The comparisons sometimes have the apparent advantage of offering a qualitative "yes-no" test of model skill: either a tracer appears in measurable quantity at a particular location as observed, or it does not.

[3] This type of comparison raises the question of whether it is not possible to deal more directly with the model/data difference? That is, to the extent that there exist inevitable quantitative discrepancies between a model "forecast" and one or more of the observations, can one undertake the systematic modification of model elements so as to improve the result or to diagnose particular model errors? This question is the heart of the so-called inverse problem: the deduction of parameters or controls that best render a model consistent within error bars with observations of any kind [*Wunsch*, 1996] (hereinafter referred to as W96). On a very different space scale, considerable success has been had recently in the introduction of "purposeful" tracers [e.g., *Ledwell et al.*, 1998] from which various mixing parameters are deduced. This, too, is a form of inverse problem. Yet another type of transient tracer behavior is that owing to statistical (stochastic) fluctuations in the tracer boundary conditions, where inferred large-scale patterns thought to reflect the structure of the flow field may in fact be random walk elements of the accumulating tracer.

[4] In a more general context the distribution of passive scalars C, whether nominally steady or fully transient, are functions of a vector of model parameters $\mathbf{p}$, which usually will include the flow field $\mathbf{v}$, mixing parameters κ, bottom topography, sources and sinks, and the like, the tracer initial conditions $C_I(\mathbf{r}, \mathbf{t} = 0)$, and boundary conditions $C_B(\mathbf{r} = \mathbf{r_B}, t)$, as well as other quantities (e.g., the initial conditions on the flow field). We can write generally,

$$C(\mathbf{r}, t) = F(\mathbf{p}, C_B, C_I, \mathbf{r}, t). \tag{1}$$

Model "testing" [e.g., *England and Maier-Reimer*, 2001] consists of computing C in a model and comparing the results with observations $C(\mathbf{r}_i, t)$ and asking whether the model/data differences,

$$\tilde{C}(\mathbf{r}_i, t_i) - C(\mathbf{r}_i, t_i), \tag{2}$$

are sufficiently small (in some sense that must be defined explicitly) that the model may be deemed to be consistent with the observations. There is no restriction in practice to passive tracers or scalar fields: identical statements would apply to testing a model against, for example, velocity or altimeter measurements or active scalar fields such as temperature. The most difficult issue is determining which of the inevitable differences is most important. It is far from clear, a priori, for example, whether model/data discrepancies in the quasi-steady temperature or salinity field are a more or a less significant or troublesome test of a model than discrepancies in a tritium or carbon transient field.

0148-0227/02/2001JC000797$09.00

[5] The inverse problem is more ambitious: it begins by determining the differences (equation (2)). Then to the degree that the differences are found to be larger than observational error would permit, one seeks to assign systematically changes to $\mathbf{p}$, C_B, C_I so as to the render the so-modified model consistent with the observations. For systems in which distributions are at least nominally steady, both the concepts and underlying methods are identical; one merely suppresses the index t in (2), and there is usually a reduction in the size of the system to be studied but no other fundamental distinction.

[6] Indeed, some controversy has lingered over the large-scale oceanic applications of transient tracers from the suggestion that the complexity of their quantitative use outweighs the information gained. A long oceanographic history exists of using approximately steady natural tracers such as silica, or phosphate, or salinity to make inferences about the general circulation. Employment of these tracers is an easy extension of conventional hydrographic work, and they have been used quantitatively, for example, in inverse analyses (e.g., W96). In contrast, when introducing transient tracers, the temporal variability usually renders the data a much smaller fraction of the total degrees of freedom, and if used in a model, the number of possible reasons for data/model discrepancies is very large. That is, even in the qualitative "yes-no" limit, a model can fail to reproduce qualitatively a transient tracer distribution because (1) the surface boundary conditions were incorrect either locally or at long distances and much earlier times, (2) the model mixed layer was inadequate, (3) the model failed to convect at the right place at the right time or to the correct depth, (4) the interior flow field or mixing processes in the ocean are inadequately represented, or all of these in concert. A failure at any stage along the tracer trajectory, from surface injection through along-track advection and mixing, can produce major distribution errors everywhere downstream for all finite time with the major possibility that the ultimate cause is misidentified because the error occurred long ago and far upstream.

[7] In addition to their use in determining flow and mixing parameters, the specific oceanographic applications of transient tracers are varied. Those such as the chlorofluorocarbons (CFCs) are unmatched in their ability to demonstrate the existence of a water property transfer from one part of the ocean to another [e.g., *Weiss et al.*, 1985], although most of this use is purely qualitative ("a water path of some kind existed, at some time in the past, from A to B"). More quantitatively, they are used to calculate so-called ventilation times: "the" interval since a water mass was last exposed to the atmosphere, both very near-surface and in the global circulation [see, e.g., *Broecker and Peng*, 1982; *Jenkins*, 1987], and tracers have been used many times to construct useful scenarios of how the ocean is behaving.

[8] A related, but different, application of transient and age tracers is their use in idealized form to diagnose GCMs without necessarily making any comparison at all to observed fields; recent examples are given by *Hirst* [1999], *Delhez et al.* [1999], and *Khatiwala et al.* [2001]. In this application one can define a number of fluid "ages," including some based upon purely hypothetical, i.e., unobservable, quantities (e.g., the tracer concentrations just prior to a mixing event). These calculations are both interesting and valuable as a way of labeling and understanding elements of the fluid flow; unfortunately, what is possible in a model is often not always even conceivable with observations, with their necessarily sparse (space and time) distributions and inevitable noise.

[9] The purpose of this note is to take a step toward providing an answer to the question "What is the information content of observable transient tracers?" by exploring a number of generic analytical and simple numerical forward examples. Although there is some applicability to the use of theoretical tracer diagnostics in numerical models, that is a separate subject, and the emphasis here is primarily on quantities at least analogous to those that one might hope to measure in nature. The primary motivation has been to understand the extent to which observed transient tracers in general, and age tracers in particular, can produce information or constraints on the oceanic general circulation. As we will show, considerable care is actually required to distinguish properties of the oceanic circulation that are fundamental flow properties from those that are directly dependent upon the details of the particular tracer being used. It is a truism of inverse modeling that a full understanding of the forward or direct problem is a prerequisite to any further progress, and it is primarily to the forward problem that we look here.

[10] Standard transient tracer forward, or direct, problems are often associated with the solution of an advection/diffusion equation of type

$$\frac{\partial C}{\partial t} + \mathbf{v} \cdot \nabla C - \nabla(\kappa \nabla C) = -\lambda C + q', \tag{3}$$

where $\mathbf{v}$ is the three-dimensional flow field, κ is a mixing tensor defined in some suitable coordinate system, λ is a decay constant, and q' is a generalized source/sink. Equation (3) is solved subject to a set of initial conditions,

$$C(t = 0, \mathbf{r}) = C_0(\mathbf{r}), \tag{4}$$

where $\mathbf{r}$ is the spatial coordinate vector, and a set of boundary conditions, either of the concentration,

$$C(t, \mathbf{r}_B) = C_B(t, \mathbf{r}_B), \tag{5}$$

or flux

$$\frac{\partial C(t, \mathbf{r}_B)}{\partial \mathbf{n}} = C'_B(t, \mathbf{r}_B), \tag{6}$$

type where $\mathbf{r} = \mathbf{r}_B$ defines the boundary coordinate (typically the sea surface but including any "open" boundary of the model through which inflow can occur) and $\mathbf{n}$ is a unit normal. In physical oceanographic studies the flow field $\mathbf{v}$ is commonly obtained from a stored time history of a GCM and (3) is solved "off-line" (defining, then, the GCM as "on-line"). The need to introduce models such as (3) in addition to the GCM itself is already an added complication of transient tracers: observations of $\mathbf{v}$ or of temperature or salinity measure state variables of the GCM directly, and their interpretation does not require the intervention of a second model.

[11] With $\mathbf{v}$ and κ known, (3) is a linear partial differential equation of somewhat deceptive simplicity. Despite all of the interest in the use of oceanic tracers, there is surprisingly little interpretive theory available.

[12] This paper emphasizes Green function and related step (or "Heaviside") responses. There are two reasons for this focus: (3) is linear in C, and Green functions provide a general solution for arbitrary boundary and source functions of time and space. They also provide a powerful and flexible general approach to the linear inverse problem [e.g., *Wunsch*, 1988, 1996; *Gray and Haine*, 2001] and permit an easy derivation of the equivalent adjoint (Lagrange multiplier) approach to assimilation of such data, although that specific application is not pursued here. Responses to Heaviside function forcing provide a convenient analytic transition from transient to steady tracers. (The step response can always be derived from the Green function and vice versa; the Green function is often somewhat easier to use but potentially more difficult to interpret.)

[13] The discussion here is generally restricted to observations for which equations similar to (3) are appropriate, the

flow field is large-scale and very simple, and the initial tracer distributions are also large-scale, relative to the flow field. We will, however, discuss the age tracer equation, one which is considerably more complex. Study of the statistical behavior of tracers in fully turbulent flow is a large subject in its own right, wholly neglected here; recent reviews are given by *Wahrhaft* [2000] and *Shraiman and Siggia* [2000]. A small literature [e.g., *Kay*, 1997] exists on tracers in nonturbulent but time-dependent flows; these are also omitted here. Even comparatively simple flows, in the presence of tracer distributions distributed initially on scales small with respect to variations in the flow, lead to the study of tracer chaos [*Ottino*, 1989]. The strategy here however, is to explore some apparently simple cases, for example, where analytical solutions are available, to produce a qualitative description of anticipated transient tracer behavior with a view toward understanding the most basic interpretation. We end (in Appendix B) with a brief excursion into the large realm of stochastically forced tracer problems.

2. One Dimension

2.1. Analytic Reference Solutions

[14] A simple situation, already exhibiting some of the major issues, is that of a transient tracer in a one-dimensional "pipe" flow with steady advection velocity w and constant κ governed by

$$\frac{\partial C_1}{\partial t} + w\frac{\partial C_1}{\partial z} - \kappa\frac{\partial^2 C_1}{\partial z^2} = -\lambda C_1 + q_s'(t,z),\ z \le 0. \tag{7}$$

Although to deal with realistic situations, we need to shift to numerical methods, it is helpful to examine first some of the possible analytical solutions to obtain a known framework and test solutions. Even this one-dimensional case proves surprisingly complicated.

[15] In practice, numerous tracers are used. Some are stable ($\lambda = 0$, e.g., ^{3}He); some lack interior sources ($q_s' = 0$, e.g., tritium, ^{3}H); some have only interior sources (e.g., ^{3}H-produced ^{3}He); some are used with surface flux boundary conditions and others with concentration boundary conditions; most enter at the sea surface, but a few (e.g., radon, terrigenic ^{3}He) enter from the seafloor; and some are in quasi-steady state (prebomb radiocarbon, ^{14}C), while others (e.g., CFCs, ^{3}H) are still undergoing strong transients. Then there are "derived" tracers, such as the "age tracer" calculated from ^{3}H/^{3}He or the ^{14}C/^{14}N pairs, which satisfy a nonlinear equation and not (7), and there is a hypothetical perfect age tracer that does satisfy an equation of the form of (7) and is useful in numerical model diagnostics.

[16] It is neither practical nor fruitful to produce solutions for every conceivable condition, but we can select a few representative cases. Here we focus on the behavior of tracers analogous to the ^{3}H/^{3}He or ^{14}C/^{14}N pairs and which is directly applicable to a variety of others (e.g., the CFCs). Tritium, which we will call, generically, the "parent," C_1, obeying (7), decays with a half-life of about 12 years into ^{3}He, called the "daughter," C_2, which then satisfies an equation

$$\frac{\partial C_2}{\partial t} + w\frac{\partial C_2}{\partial z} - \kappa\frac{\partial^2 C_2}{\partial z^2} = \lambda C_1,\ z \le 0, \tag{8}$$

with the surface boundary condition $C_2(t, z = 0) = 0$ representing outgassing of ^{3}He to the atmosphere. The term λC_1 in (8) makes the daughter depend upon the parent C_1, but the parent equation does not depend upon the daughter product. We begin by studying certain limiting cases of the parent alone.

2.1.1. Pure advection. [17] This case is of some interest when we examine idealized age tracers. Set $\kappa = 0$ and $w < 0$ and let the source be a boundary flux $q_s'(t) = S_0 q_0(t)\delta(z)$. Then the solution is

$$C_a^f(t,z) = S_0\frac{\exp[-(\lambda/w)z]}{w}\int_{-i\infty+\gamma}^{i\infty+\gamma}\exp[pt - (p/w)z]\tilde{q}_0(p)dp,\ z, w < 0$$
$$C_a^f(t,z) = 0,\ z > 0,\ w < 0, \tag{9}$$

written as an inverse Laplace transform, where $\tilde{q}(p)$ is the transform of the source time function. The Green function, with $q_o(t) = \delta(t)$, is

$$C_{Ga}^f(t,z) = \frac{S_0}{w}\exp(-\lambda z/w)\delta(t - z/w), w < 0, \quad z < 0,$$
$$C_{Ga}^f(t,z) = 0, w, \quad z > 0, \tag{10}$$

a simple advected pulse. If the source in time is a Heaviside function, $q(t) = H(t)$, we obtain

$$C_{Ha}^f(t,z) = \frac{S_0}{w}\exp(-\lambda z/w)H(t - z/w), w, \quad z < 0,$$
$$C_{Ha}^f(t,z) = 0, z > 0, w < 0. \tag{11}$$

With a flow down the pipe the concentration arrives as a discrete front at $t = z/w$ but diminishing with distance (time) owing to the decay. (I will use subscripts G to denote Green function solutions, H to denote Heaviside response solutions, a for purely advective, d for purely diffusive, and f and c to denote flux and concentration boundary condition solutions, respectively.)

2.1.2. Pure diffusion. [18] This problem, with $w = 0$ and $\lambda = 0$, in various specific forms, is well known [e.g., *Morse and Feshbach*, 1953, section 7.4; *Carslaw and Jaeger*, 1986] and of no special interest here. There is, however, one useful point. Consider an infinitely deep ocean with boundary at $z = 0$, where a step change, $C_0H(t)$, is made to the tracer concentration. *Carslaw and Jaeger* [1986, pp. 134–135] show that the appropriate solution is

$$C_{Hd}^c(t) = C_0\mathrm{erfc}\left[-z/\left(2\sqrt{\kappa t}\right)\right], \quad z < 0, \tag{12}$$

where erfc is the complementary error function. The purpose of displaying this solution is that it illustrates a mathematical issue present in the more complicated configurations taken up below: $C(t)$ responds instantaneously, although weakly, at any finite value of z to a tracer disturbance to $z = 0$, $t = 0$. Equation (12) suggests that the signal velocity from the surface to any finite depth is infinite, a physical impossibility. The resolution of the paradox is the recognition [see *Morse and Feshbach*, 1953] that the advection/diffusion equation is valid at distance z only after a time longer than a finite propagation time normally given by the fastest possible wave in the system (commonly the speed of light or the speed of sound); a more correct description is via the so-called telegrapher's equation. In the present situation, where equations such as (7) are based upon the Reynolds analogy for turbulent mixing rather than upon a rigorous invocation of molecular processes, the appropriate delay time is obscure. There is a clear discussion by *Monin and Yaglom* [1975, pp. 678+]. The main point here is that it would be a poor idea to calculate a "ventilation time" or equivalent from the first appearance of a tracer at a fixed point as the answer would depend sensitively upon the detection threshold.

2.1.3. Tritium-like surface source. [19] To be specific, take $w > 0$ and zero initial conditions $C_1(t = 0, z) = 0$ so that if the sea surface is $z = 0$, the situation is one of upwelling toward the surface. In the present case we are interested primarily in surface

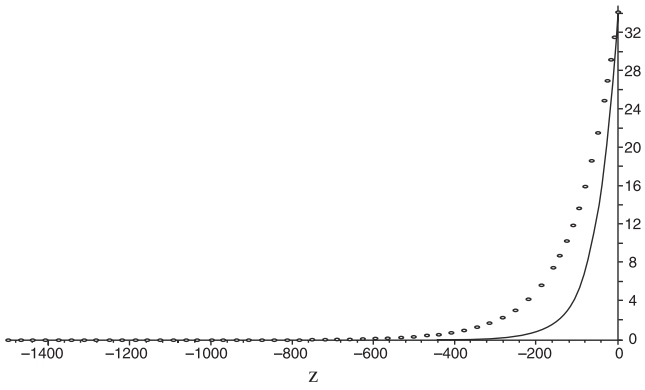

Figure 1. Solution from (21) (dashed curve) for $w < 0$ and from (22) for $w > 0$. In this diffusive range ($w = \pm 10^{-6}$ m s^{-1}, $\kappa = 10^{-4}$ m^2 s^{-1}, and $\lambda = 1.9 \times 10^{-8}$ s^{-1}) the asymmetry with w is not particularly marked.

sources. Let the surface flux be taken as the Robbins boundary condition,

$$-\kappa \frac{\partial C_1(0,t)}{\partial z} + wC_1(0,t) = \delta(t), \tag{13}$$

i.e., combining the diffusion and advection contributions, envisioned as owing to a surface mixed layer. The solution is subject to the boundedness condition,

$$C_1(t,z) \to 0, \quad z \to -\infty, \tag{14}$$

with initial condition $C_1(0, z) = 0$. Then the boundary Green function can be inferred from the solution given by *Lee* [1999, equation (7.78)] (letting his $x \to -z$, $\bar{v} \to -w$, $D \to \kappa$, $R = 1$) and is

$$C^f_{1G}(z,t) = \frac{w^2}{\kappa}\exp(-\lambda t) \cdot \left\{ \sqrt{\frac{\kappa}{\pi w^2 t}} \exp\left[-\frac{(-z+wt)^2}{4\kappa t} \right] - \frac{1}{2}\exp\left(-\frac{zw}{\kappa}\right) \cdot \operatorname{erfc}\left[-\frac{(z+wt)}{2\sqrt{\kappa t}} \right] \right\}, \quad z < 0 \tag{15}$$

and which, as with Green functions in general, can be convolved with a source having an arbitrary time history.

[20] For a concentration boundary condition at $z = 0$, instead of a flux, the Green function [*Lee*, 1999, equation (7.39)] is even simpler:

$$C^c_{1G}(t,z) = \frac{-z}{2\sqrt{\pi\kappa}t^{3/2}} \exp\left[-\lambda t - \frac{(-z+wt)^2}{4\kappa t} \right], t \geq 0, z < 0. \tag{16}$$

As is generally true for boundary Green functions, the general boundary concentration solution is obtained by convolution,

$$C^c(t,z) = \int_0^\infty \frac{-z}{2\sqrt{\pi\kappa}t^{3/2}} \exp\left[-\lambda t' - \frac{(-z+wt')^2}{4\kappa t'} \right] C_0(t-t')dt'. \tag{17}$$

These solutions have some mathematically interesting features discussed by *Reddy and Trefethen* [1994]. In technical terms the differential operator is "nonnormal." This structure manifests itself in the present solution through the qualitative change in solution transient behavior when w changes sign. Another useful reference solution [*Lee*, 1999, equation (7.36)] is that for a unit step, $H(t)$, in concentration at $z = 0$,

$$C^c_{1H}(t,z) = \tfrac{1}{2}\exp\left(-\tfrac{wz}{k}\right)\exp\left(\tfrac{\sqrt{w^2+4\lambda}}{2k}z\right) \operatorname{erfc}\left(-\tfrac{z+\sqrt{w^2+4\kappa\lambda t}}{\sqrt{4\kappa t}}\right) + \tfrac{1}{2}\exp\left(-\tfrac{wz}{\kappa}\right)\exp\left(-\tfrac{\sqrt{w^2+4\lambda}}{2\kappa}z\right) \cdot \operatorname{erfc}\left(-\tfrac{z-\sqrt{w^2+4\kappa\lambda t}}{\sqrt{4\kappa t}}\right) \quad z < 0, w > 0. \tag{18}$$

[21] For some purposes, nondimensionalization is useful, but there is a remarkably large number of timescales/space scales that can appear in these problems, which is a major issue in their interpretation during the transient phase. Natural internal timescales and space scales are $T_1 = \kappa/w^2$ and $L_1 = \kappa/w$. This timescale is that required to establish fully a boundary layer of thickness L_1, but one which exists only if $w > 0$ when $z < 0$. Another possible pair is $T_2 = 1/\lambda, L_2 = \sqrt{\kappa/\lambda}$, based upon the decay time, and a third is the combination scale $T_3 = \kappa/(w^2 + 4\lambda\kappa), L_3 = \kappa/\sqrt{w^2 + 4\lambda\kappa}$. Take dimensional values $\kappa = 10^{-4}$ m^2 s^{-1}, $w = 10^{-7}$ m s^{-1} (roughly consistent with the global values of *Munk and Wunsch* [1998]), and $\lambda = 1.77 \times 10^{-9}$, with the choice of λ corresponding to the decay constant for ^{3}H. Then ($T_1 = 318$ years, $L_1 = 1000$ m), ($T_2 = 18$ years, $L_2 = 238$ m), and ($T_3 = 44$ years, $L_3 = 118$ m). If the source history $C_0(t)$ has its own characteristic time T_4, that will also enter. Two more timescales can be based upon the diffusion time over the full water column; $T_5 = h^2/\kappa$ and the advection time $T_6 = h/w$. All of these scales may, but will not necessarily, appear in the problem, with an importance dependent upon the problem details (e.g., the sign of w: whether advection competes with or reinforces, diffusion) as well as their relative magnitudes (e.g., if $w < 0$, and the advection time T_6 is less than the diffusion time, T_5 may then be irrelevant). *Butkovskiy* [1982] provides an extended list of Green functions useful for problems in oceans of finite depth h.

[22] The existence of all these timescales, plus many others in the two- and higher space-dimensional problem, make quite treacherous, if interesting, the use of tracers for oceanographic inference, particularly if the inference is to be from simplified temporal or spatial changes without actual integration of the governing equation. The very long half-life for radiocarbon (5500 years) would further render extremely doubtful any assumption that the ocean circulation could have remained constant enough for a steady state distribution to have been reached, and one must try to understand the effects of temporal changes on the present-day observed distributions. Thus timescale T_7 for significant change in the flow field (and possibly T_8 for mixing rate changes) must also be borne in mind.

[23] Much of the (very large) literature on inferences about the ocean circulation from transient tracers is built upon use of (16)–(18) and various generalizations under the assumption that one of the timescales dominates the solution. The reliability of the resulting inferences has to be evaluated on a case-by-case basis. It is helpful therefore to examine some even simpler limits.

2.1.4. Steady state. [24] On timescales long compared to T_1, with the source or surface boundary condition held fixed, the step source solutions asymptote to a steady state obtained by letting $t \to \infty$ in the transient solutions while keeping $|z|$ bounded; this result connects transient and steady tracers. The asymptote is, however, more readily found by assuming the steady state has been reached and then solving directly.

[25] Suppose there is a steady source located at $z = 0$. Then the governing equation is

$$w\frac{\partial C_1}{\partial z} - \kappa\frac{\partial^2 C_1}{\partial z^2} = -\lambda C_1 + S_0\delta(z). \tag{19}$$

Write

$$C_1(z) = \int_{-\infty}^{\infty} \tilde{C}_1(m) e^{2\pi i m z} dm, \tag{20}$$

and we obtain by substitution into (19) the Fourier transform of the δ function and simple contour integration,

$$\begin{aligned} C_{1G}(z) &= \frac{-S_0}{w(1+4\lambda\kappa/w^2)^{1/2}} \exp\{m_+ z\}, \\ m_+ &= \frac{w}{2\kappa} - \frac{w}{2\kappa}\left(1+\frac{4\lambda\kappa}{w^2}\right)^{1/2}, \quad z<0, w<0. \end{aligned} \tag{21}$$

$$\begin{aligned} &= \frac{S_0}{w(1+4\lambda\kappa/w^2)^{1/2}} \exp\{m_- z\}, \\ m_- &= \frac{w}{2\kappa} + \frac{w}{2\kappa}\left(1+\frac{4\lambda\kappa}{w^2}\right)^{1/2}, \quad z<0, w>0. \end{aligned} \tag{22}$$

[26] Note (Figure 1) the dependence upon the sign of w, with the downward advection reinforcing diffusion and producing a larger concentration than when advection and diffusion are opposed. In the former case the concentration would be uniform if $\lambda = 0$. These expressions are the limit as $t \to \infty$ of (18), using erfc $(\infty) = 0$, erfc $(-\infty) = 2$. The limit $\kappa \to 0$ is a singular one as it reduces the order of the differential equation. For the present parameter range the difference with the sign of w is only quantitatively significant.

[27] The vertical property flux, $F = wC - \kappa \partial C/\partial z$, below the surface is

$$F = \frac{-C_0}{2}\left(1 - 1\Big/\sqrt{1+\frac{4\lambda\kappa}{w^2}}\right) \exp\left[\frac{w}{2\kappa}\left(1+\sqrt{1+\frac{4\lambda\kappa}{w^2}}\right)z\right], z<0, \tag{23}$$

and which vanishes if $\lambda\kappa = 0$. This expression is of interest when one examines the diagnosis of property fluxes from box models. By one definition the mass flux is w (taking density $\rho = 1$), there being no diffusive mass flux, while the property flux is (23), thus demonstrating the fundamental distinction between mass and property fluxes.

2.1.5. Achieving a steady state. [28] The temporal evolution of the various solutions toward a steady state or quasi-static behavior is surprisingly complex. Note that in the parameter range we are using for nominal values, T_1 exceeds 300 years and would be the time required to establish the main boundary layer scale κ/w. This timescale is very long relative to, for example, any of the bomb transients or the CFC transient time. Assumption of near-steady state for these tracers is probably a poor idea. Consider, for example, the Green function (16) for a ^{3}H-like surface source and $w > 0$. Then the depth of the concentration maximum at time t is at

$$z_m = \frac{wt}{2}\left[1 - \left(1+\frac{8\kappa t}{w^2 t^2}\right)^{1/2}\right]. \tag{24}$$

In the diffusion limit, $t \ll 8\kappa/w^2$ and $z_m \sim -\sqrt{2\kappa t}$, and in the advection limit, $8\kappa/w^2 \ll t$ and $z_m \sim -2\kappa/w$ independent of time. For the standard parameters here the transition between the two limits occurs after about 300 years, suggesting great care is required in interpreting the observed depth of bomb products as being dominantly either a diffusive or advective process.

2.1.6. Interior ^{3}H-like source. [29] *Kelley and van Scoy* [1999, equation (3)] gave a solution for an initial, Gaussian interior ^{3}H distribution centered at $z = z_0$ below the surface modified for a surface no-flux condition. They envisioned the ^{3}H to appear below the sea surface by subduction at a higher latitude, followed by lateral transfer along neutral surfaces, and then studied its subsequent local, purely vertical, evolution. It is easy to see, however, that their solution is valid only for times such that neither diffusion nor advection has time to carry significant tracer to the local sea surface (because it does not actually satisfy their no-flux surface boundary condition). They assumed that the behavior of the ^{3}H transient in the North Pacific is effectively a δ function, entering at a finite depth, z_0, which gives rise to an approximate Green function of form (present notation)

$$C_{1G}(t,z) = \frac{S_0}{(\kappa t)^{1/2}} \exp\left[-\lambda t - (z - z_0 - wt)^2/(4\kappa t)\right], \tag{25}$$

not satisfying the surface conditions. In this solution the role of w is only to provide a bodily translation of the center of mass of the dye patch with all other time evolution controlled solely by diffusion. This solution is the appropriate one for an infinite domain initial value problem but not for a fixed depth source. That this is true can be seen by noting that if $w < 0$, with a sustained source at a fixed depth, advection competes against the outward diffusion of C_1 above the source, but below the source, w reinforces the diffusive effects in carrying tracer away. This asymmetry about the source is not reflected in (25).

2.2. Oddities of the One-Dimensional Steady State

[30] The one-dimensional steady-state balance,

$$w\frac{\partial C_1}{\partial z} - \kappa\frac{\partial^2 C_1}{\partial z^2} = 0, \tag{26}$$

has been widely used in oceanography, particularly since *Munk* [1966]. The general solution is

$$C_1 = Ae^{(w/\kappa)z} + B. \tag{27}$$

Let the surface condition be $C_1(z = 0) = C_0$. When working with data, it has usually been assumed, implicitly, that the fluid depth, $z = -h \to -\infty$, demanding $B = 0$ to obtain concentration decay with depth. If, however, the boundary condition at the seafloor is that of no diffusive flux,

$$\kappa\frac{\partial C_1}{\partial z}\bigg|_{z=-h} = 0, \tag{28}$$

the solution is $C_1(z) = C_0$, independent of the sign of w. Because of the size of T_1, if $w > 0$, the asymptote can take a very long time to achieve.

[31] If, on the other hand, we require no net flux at $z = -h$,

$$\left(wC_1 - \kappa\frac{\partial C_1}{\partial z}\right)_{z=-h} = 0, \tag{29}$$

the solution is

$$C_1(z) = C_0 e^{(w/\kappa)z} \tag{30}$$

and is extremely sensitive to the sign of w (in this solution there is no property flux at any depth). Neither upper nor lower boundary condition is readily imposed in a true one-dimensional system; one must assume a higher-order boundary layer or reservoir at each end to absorb w, but because all numerical

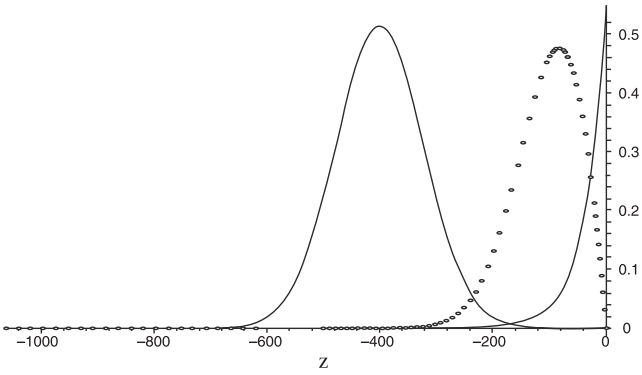

Figure 2. Daughter (helium-like) Green function (multiplied by 10^6) at time $t = 10^6$ s (equation (31)) for $w = -10^{-5}$ m s^{-1} and $\kappa = 10^{-4}$ m^2 s^{-1} (dashed curve) and at time $t = 3 \times 10^7$ s (about 1 year). The putative source was placed at $z_0 = -100$ m at $t_0 = 0$. In the solid curve the maximum has been carried downward by advection. The maximum continues to grow from the ^{3}H source. Topmost solid line is repeated from Figure 1.

codes require something be done at a finite depth, one needs to be aware of the great sensitivity in the steady state of the solution to the boundary condition choice.

2.3. Helium-Like Tracer

[32] We turn now to consideration of daughter tracers. In the ^{3}H/^{3}He or ^{14}C/^{14}N problems the appropriate source for the daughter product is vertically distributed in the interior, subject to a boundary condition of zero concentration at $z = 0$ (for ^{3}He). For the daughter, take an interior source $\delta(z - z_0)\,\delta(t - t_0)$, with the resulting Green function required to satisfy the surface boundary condition $C_1 = 0$. The appropriate solution can be obtained by using a Laplace transform in time, by using a Fourier transform in z, and by doing several pages of algebra, with result

$$C^c_{2G}(t-t_0,z,z_0) = \frac{\sqrt{\kappa}}{2\sqrt{\pi(t-t_0)}}\exp\left[\frac{w(z-z_0)}{2\kappa} - \frac{w^2(t-t_0)}{4\kappa}\right] \cdot\left\{\exp\left[-\frac{(z-z_0)^2}{4\kappa(t-t_0)}\right] - \exp\left[-\frac{(z+z_0)^2}{4\kappa(t-t_0)}\right]\right\}, \quad z<0, t_0<t. \tag{31}$$

Note that in (31) the effect of w changes sign in one of the terms with $z - z_0$. This Green function is displayed in Figure 2 for both positive and negative w and with $z_o = -100$ to exaggerate the boundary effect. The maximum moves downward much more rapidly when κ and w are reinforcing. This solution perhaps has some utility, too, for a "purposeful tracer" [e.g., *Ledwell et al.*, 1998] subject to a zero-concentration boundary condition, introduced at a finite depth over a finite time interval, and then integrated over both horizontal dimensions to remove the short scale. Apart from the vertical movement, the asymmetry with w is not very conspicuous.

[33] Modification of the solution so as to accommodate the *Kelley and van Scoy* [1999] interior ^{3}H source and zero-concentration boundary condition is straightforward (multiply (31) by exp $[\lambda(t - t_0)]$). The appropriate zero-flux boundary condition solution, with

$$-\kappa\frac{\partial C(t,z=0)}{\partial z} + wC(t,z=0) = 0, \tag{32}$$

can also be obtained, but is quite intricate, resulting from a tedious exercise in Laplace transform inversion, and is not shown here.

3. Age Tracers: Hypothetical and Real

[34] Equations (7) and (8) are a coupled linear system. In some applications [e.g., *Jenkins*, 1987, 1988; *Robbins and Jenkins*, 1998] it has become customary to produce an equation in a single variable, the tracer "age," defined as

$$\tau = \frac{1}{\lambda}\ln\left(1 + \frac{C_2}{C_1}\right). \tag{33}$$

The motivation is clear: for an ordinary nonfluid system the classical parent-daughter pair (e.g., in radiocarbon dating),

$$\frac{\partial C_1}{\partial t} = -\lambda C_1,\ \frac{\partial C_2}{\partial t} = \lambda C_1,$$

has solution,

$$C_1 = C_0\exp(-\lambda t), C_2 = C_0[1-\exp(-\lambda t)], C_1(0) = C_0, C_2(0) = 0. \tag{34}$$

When substituted into (33), one has $\tau = t$, and the equation governing τ is

$$\frac{\partial \tau}{\partial t} = 1,\ \tau(0) = 0, \tag{35}$$

and so τ is the time since the transient started.

[35] In the fluid system the differential equation for τ is much more complex (see *Jenkins* [1987, appendix] or *Doney et al.* [1997] for a derivation):

$$\frac{\partial \tau}{\partial t} = \kappa\frac{\partial^2\tau}{\partial z^2} - w\frac{\partial\tau}{\partial z} + \kappa\frac{\partial\tau}{\partial z}\frac{\partial}{\partial z}\{\ln[C_1(C_1+C_2)]\} + 1, \tag{36}$$

a somewhat problematic relation because of the nonlinear term on the right-hand side. This nonlinearity occurs because τ involves the ratio of the parent and daughter tracers, each of which satisfies its own advection/diffusion equation. Nonlinearity is the source of much difficulty in solutions to the forward, and hence, the inverse, problems. The chief virtue of the nonlinear transformation is that both the surface boundary condition and the source strength are known perfectly (but for ^{3}He the surface boundary condition is also $C_2 = 0$ exactly). The greatest attraction to the use of τ is its identification as a "ventilation" time, the time since fluid was apparently in contact with the sea surface.

[36] So-called perfect age tracers satisfying the purely linear form of (36),

$$\frac{\partial\tau}{\partial t} = \kappa\frac{\partial^2\tau}{\partial z^2} - w\frac{\partial\tau}{\partial z} + 1, \tag{37}$$

are sometimes used as theoretical diagnostics of model behavior and in three-dimensional generalization are commonly computed and analyzed in numerical models. Setting $\kappa = 0$ produces a special case of the perfect age tracer, which is distinguished here as a "perfect advective" age tracer. Conventionally, radiocarbon dates are computed from the parent alone, relative to a fixed surface reservoir ^{14}C concentration. Because the evolution equation for ^{14}C is very different than that for τ, radiocarbon ages in the ocean cannot be expected to coincide with those computed from a τ based upon hypothetical knowledge of ^{14}N concentrations. For

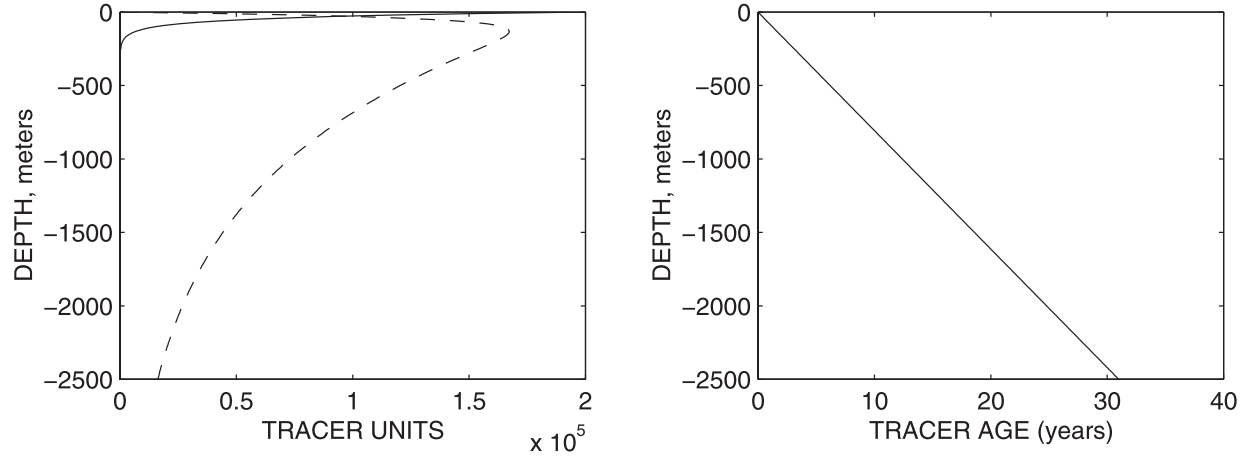

Figure 3. (left) Steady state tritium (solid) and helium profiles (dashed) with a constant surface tritium source. (right) The age τ in this steady state with no boundary layer character.

purposes of simplifying the discussion in this theoretical paper we will maintain the fiction that ^{14}N concentrations are known.

3.1. Perfect Advective Age Tracers

[37] Let there be a steady parent tracer source at $z = 0$,

$$C_1^c(t, z = 0) = S_0 H(t), \tag{38}$$

and suppose that there is no diffusion, $\kappa = 0$. Then the parent solution is (11). The corresponding daughter solution is

$$C_2^c(t, z) = \frac{S_0}{w}\left[1 - \exp\left(-\frac{\lambda}{w} z\right)\right] H\left(t - \frac{z}{w}\right),\ z,\ w < 0 \tag{39}$$

One readily confirms that

$$\tau = \frac{z}{w},\ t > \frac{z}{w},\ z,\ w < 0, \tag{40}$$

which, indeed, is the time since the tracer front left $z = 0$ and which would follow directly from solution of (37) with $\kappa = 0$. Here τ does have a very simple interpretation as the time since residence at the surface and has been much used as a qualitative measure in observations, simply ignoring the effects of diffusion.

3.2. Time-Evolving Age Solution

[38] An analytic solution, expressed as a convolution integral, for the parent-daughter age calculation can be obtained by using (16) as a source term and the daughter Green function (31), calculating the age from the definition of τ. The result is sufficiently cumbersome that direct numerical integration seems preferable and is taken up presently.

3.3. Steady State Real Age Tracer

[39] A more tractable problem, but still an interesting one, is that for the age in a hypothetical steady state with the parent source at $z = 0$. In that case the solution for the parent is given by (21) and (22) with $z_0 = 0$. The daughter equation is

$$w\frac{\partial C_2}{\partial z} - \kappa\frac{\partial^2 C_2}{\partial z^2} = \lambda C_1. \tag{41}$$

One finds

$$\begin{aligned} C_2(z) &= \frac{\lambda S_0}{w^2(1 + 4\lambda\kappa/w^2)^{1/2}[m_-(\kappa/w) - 1]m_-} \\ &\quad \cdot\left[\exp\left(\frac{w}{\kappa} z\right) - \exp(m_- z)\right],\ z < 0, \\ m_- &= \frac{w}{2\kappa} + \frac{w}{2\kappa}\left(1 + \frac{4\lambda\kappa}{w^2}\right)^{1/2},\ w > 0, \end{aligned} \tag{42}$$

where the boundary condition at $z = 0$ has been enforced; this solution is the $t \to \infty$ limit of (31). C_1 and C_2 are displayed in Figure 3 for the same dimensional parameters, $\kappa = 10^{-4}$ m^2 s^{-1}, w = 10^{-7} m s^{-1}, and $\lambda = 6.3 \times 10^{-8}$. One has then

$$\begin{aligned} \tau &= \frac{1}{\lambda}\ln\left\{1 + \frac{\lambda}{w(1 + 4\lambda\kappa/w^2)^{1/2}[1 - m_-(\kappa/w)]m_-}\right. \\ &\quad \left.\cdot\left[1 - \exp\left(\frac{w}{\kappa} z - m_- z\right)\right]\right\} \\ &= -\frac{w}{2\lambda\kappa}\left(\sqrt{1 + \frac{4\lambda\kappa}{w^2}} - 1\right) z, \quad z < 0, \quad w > 0, \end{aligned} \tag{43}$$

i.e., a straight line. Equation (43) can be confirmed to be the exact solution to the nonlinear (36), with the term in $\kappa\partial^2\tau/\partial z^2$ vanishing identically.

[40] The limit of (43) as $\lambda\kappa/w^2 \to 0$ is

$$\tau \to -\frac{z}{w}, \tag{44}$$

apparently the perfect advection limit. The reader, however, is urgently cautioned that (44) has nothing to do with the time since a fluid particle was at the surface. Rather, this is the advection time required for the high age "source" at depth to carry its value to the surface. As $\lambda\kappa/w^2 \to \infty$,

$$\tau \to -\frac{z}{\sqrt{\lambda\kappa}}, \tag{45}$$

which, because it depends upon λ, is not a property of the fluid alone. Thus the apparent age, for example, at 4000 m, in a diffusive

Table 1. Correspondence of Common Meteorological Terminology and That Used Here[a]

Meteorological Dialect	Oceanographic Dialect
Mean age	steady state age
Age spectrum	boundary Green function
Continuity equation	advection/diffusion equation plus (sometimes) higher-order terms
Incompressibility condition	continuity equation
Boundary propagator	boundary Green function
Probability density	integral of Green function
Age tracer	linearly growing boundary condition; no interior source
Linearly growing interior source	age tracer
Mixing ratio	concentration/unit mass

[a] The definitions are not universally applicable, and usage varies greatly from author to author.

ocean, derived from $^3H/^3He$ in this limit (about 300 years) would differ from that of $^{14}C/^{14}N$ (about 6400 years) because of the different values of λ, even if the physical boundary conditions were identical. This result immediately raises the question of how such results, for example, the radiocarbon age, could be interpreted as a ventilation time, depicting as it does a tracer property, rather than one purely of the fluid alone? At depth z the ratio of the diffusion time to the age is

$$\frac{z^2/\kappa}{z/\sqrt{\lambda\kappa}} = z\sqrt{\frac{\lambda}{\kappa}} \approx 2\times 10^{-4} z \tag{46}$$

for radiocarbon. At z = 1000 m the diffusion time to ventilate the water is only about 20% of the apparent radiocarbon age. By accident the two ages are comparable near z = 5000 m for the κ value used. For ^3H and ^3He the diffusion time at 1000 m is about 4 times longer than τ. At greater depths the concentration of ^3H and ^3He would be extremely small, and for these tracers one is dealing with mathematical rather than practical possibilities.

[41] In between the two limits, τ involves all of κ, w, and λ in an intricate way. Vertical advection and diffusion are of equal importance when $4\lambda\kappa/w^2 \approx 1$. For this ratio to be unity for ^3H, and using $\kappa = 10^{-4}$ m^2 s^{-1}, one has $w \approx 8\times 10^{-7}$ m s^{-1} and, for radiocarbon, $w \approx 4\times 10^{-8}$ m s^{-1}. Any much smaller values of w produce a primarily diffusive response. In the steady state, age does not have the boundary layer character of C_1 and C_2 separately. Because (40) produces a straight line age, one could define an effective advective velocity, w^*, from (43), which would be positive downward and misleading in terms of the actual physics. For an inversion, to determine w, κ, there would appear to be little gain in using (43) as opposed to either (42) or (22) or both (all depend upon w/κ and w^2/κ). Apart from ^{14}C, whether there are any useful tracers in nature actually having this steady state character under either flux or concentration boundary conditions is unclear, although one might try to so interpret the radon 228 to lead 208 series in the sediments [e.g., *Moore et al.*, 1985].

[42] In any parent-daughter pair, observations of $C_1(z)$ and $C_2(z)$ are functions of the two parameters and provide a basis for curve fitting to determine the parameters (inversion). One can use τ directly, rather than computing it from the parent and daughter; whether the gain in boundary condition accuracy is worth the complexity of a nonlinear forward (and inverse) problem is a matter of taste. If one had reduced a nonlinear system (36) to a linear coupled system (8) and (19), it would usually be regarded as a major simplifying achievement.

[43] In practice, τ cannot be measured directly but is calculated from $C_{1,2}$. Were it possible to measure τ, use of (36) would become more compelling. This conclusion about the utility of the age is somewhat at odds with the stratospheric experience [e.g., *Hall and Plumb*, 1994; *Neu and Plumb*, 1999] where the short timescale and specific geometry renders the interpretation much simpler. (Readers of the meteorological literature may find it helpful to recognize that the terminology there differs considerably from that used here. As an aid to crossing disciplinary boundaries, Table 1 offers a brief dictionary for translation of some of the meteorological dialect into the present oceanographic one, where I have tried as far as possible to adhere to the most widely accepted terminology. Note, for example, that "spectrum" conventionally implies the eigenvalue distribution of a linear operator with direct connection to Fourier representations; its meteorological use as a synonym for concentration distribution or Green function mainly serves to confuse, as one might wish to compute a wavenumber spectrum of an age distribution.)

[44] The one space dimension considered here is too simple to be a reliable guide to oceanographic inference, and we will revisit the age tracer problem in two dimensions below. A useful discussion of some of the other, practical, issues involved in using age tracers is given by *Doney et al.* [1997].

4. Discretization

[45] The above analytic solutions are useful for exploring the behavior of transient tracers in the simplest of all situations. Almost all further complications, however, including general time-dependent flows and increased dimensions, force one to numerical methods. For some purposes a discretization in space, with time remaining continuous, has its advantages. A very brief discussion of this formalism has been placed in Appendix A; we will move here directly to the more flexible, fully discrete case.

[46] A Dufort-Frankel leapfrog scheme [*Roache*, 1976, equation (3–167)] is used as

$$\begin{aligned} C_i(t+1) &= C_i(t-1) - \frac{\Delta t}{\Delta z}\left[wC_{i+1}(t) - wC_{i-1}(t)\right] \\ &\quad + \frac{2\kappa\Delta t}{\Delta z^2}\left[C_i(t) + C_{i-1}(t) - 2C_i(t-1)\right] \\ &\quad /\left(1 + 2\kappa\Delta t/\Delta z^2\right) + 2\Delta t q_i'(t) \end{aligned} \tag{47}$$

or

$$\mathbf{c}(t+\Delta t) = \mathbf{A}_1\mathbf{c}(t) + \mathbf{q}_{1s}(t), \tag{48}$$

where

$$\mathbf{c}(t) = \left\{ \begin{array}{c} \mathbf{c}(t) \\ \mathbf{c}(t-1) \end{array} \right\}, \mathbf{q}_{1s} = 2\Delta t \mathbf{q}_s'. \tag{49}$$

Notice that the state vector contains two time levels even though the original equation is first-order in time. The general solution to (48) is

$$\mathbf{c}(n\Delta t) = \mathbf{A}_1^t\mathbf{c}(0) + \mathbf{A}_1^t\mathbf{q}_{1s}(0) + \mathbf{A}_1^{t-1}\mathbf{q}_{1s}(\Delta t) + \ldots \mathbf{q}_{1s}(n\Delta t - 1). \tag{50}$$

The modifications to be made if $\mathbf{A}_1$ is time-dependent should be apparent.

5. Green Functions, Inverse Problems, and Adjoints

[47] Green functions are the natural tool for formulating tracer inverse problems as they provide a connection between a disturbance at one point and the subsequent signals at all other points. This approach was used by *Wunsch* [1988], *Mémery and Wunsch* [1990], and *Gray and Haine* [2001] to solve transient tracer problems with real data. As discussed by *Stammer and Wunsch* [1996] and *Menemenlis and Wunsch* [1997], there is an immediate connection, too, between the Green function, the so-called state transition matrix $\mathbf{A}_1$, and the problem adjoint [see also, *Holzer and Hall*, 2000]. All of this is at least implicit in the classical discussions of Green functions by, for example, *Morse and Feshbach* [1953].

[48] Consider (48) as a set of pure initial values problems with $\mathbf{q}_{1s}(t) = 0$, such that

$$\mathbf{g}^{(j)}(t+1) = \mathbf{A}_1\mathbf{g}^{(j)}(t), \tag{51}$$

subject to the initial condition $g_i^{(j)}(0) = \delta_{ij}$, i.e., the initial condition with unity in location j and 0 everywhere else. This solution represents the numerical Green function for a delta function source at position $z = z_j$, including, but not limited to, the boundary points, $j = 1, N$ (that is, the boundary Green function is included as a special case). The collection of solutions for every possible position of the source is evidently the solution to

$$\mathbf{G}(t+1) = \mathbf{A}_1\mathbf{G}(t), \;\; \mathbf{G}(0) = \mathbf{I}, \tag{52}$$

where $\mathbf{I}$ is the identity matrix. That is, the Green function $\mathbf{G}(t)$ is a matrix whose jth column corresponds to the Green function for a delta function at the corresponding z_j position. It follows immediately that

$$\mathbf{G}(t) = \mathbf{A}_1^t, \;\; t \geq 0 \tag{53}$$

Parts of the Green function for the one-dimensional case are shown in Figure 4. If one can infer the Green function, the state transition matrix is immediately known. The interpretation is that $G_{ij}(t)$ is the tracer concentration at point z_i at t from a pulse in tracer concentration at point z_j at time $t = 0$. If the pulse is delayed until time t_0, the temporal stationarity of (52) shows immediately that $\mathbf{G}(t, t_0) = \mathbf{G}(t - t_0) = \mathbf{A}_1^{t-t_0}$. Any stable system will produce a decaying response, so that $||\mathbf{G}(t)|| \rightarrow 0$, $t \rightarrow \infty$.

[49] For a flow field that is time-dependent, $\mathbf{A}_1$ is a function of t, and one readily finds that

$$\begin{aligned}\mathbf{G}(t, t_0) &= \mathbf{A}_1(t - t_0)\mathbf{A}_1(t - t_0 - 1)\ldots\mathbf{A}_1(t_0 + 1)\mathbf{A}_1(t_0) \\ &\neq \mathbf{G}(t - t_0),\end{aligned} \tag{54}$$

which involves more bookkeeping but no greater conceptual difficulty.

[50] Suppose that the tracer concentration at any given point z_j can be controlled externally with a value $q_j(t)$ (an artificial situation for this one space dimension case, but because there is only one (surface) boundary point, it is more interesting to consider the ability to inject dye at any vertical position. In two dimensions, as discussed below, the appearance of many boundary points makes the problem more physically interesting.). Then by the conventional properties of an impulse response (the Green function) we can write the time history of the vector of concentrations as the convolution,

$$\mathbf{c}(t) = \sum_{n=0}^{\infty}\mathbf{G}(n)\mathbf{q}(t-n), \tag{55}$$

using causality $\mathbf{G}(t < 0) = 0$. Typically, there is rapid decay in $\mathbf{G}(n)$ as n grows, and in practice the infinite summation in (55) is replaced by a small, finite upper limit.

[51] Equation (55) is the basis for the Green function approach to the transient tracer inverse problem. One writes the observations as $y_i(t_r) = c_i(t_r) + \varepsilon_i(t_r)$, where ε is the observational and model noise. Substituting (55) we have

$$y_i(t_r) = \sum_{n=0}^{\infty}\sum_j G_{ij}(n)q_j(t_r - n) + \varepsilon_i(t_r), \tag{56}$$

which is a conventional statement of a linear inverse problem for estimation of q_j and ε_i. The approach is very general as long as the problem is linear or linearizable; $\mathbf{G}$ lends itself to simplification and parameterization.

[52] Physically, $G_{ij}(t - t')$ represents the influence at point i of a tracer disturbance at point j at time t' earlier. Equivalently, column $\mathbf{g}_j(t - t')$ of matrix $\mathbf{G}(t - t')$ is the contribution at all points i from the earlier disturbance at point j. Conversely, row i of $\mathbf{G}(t - t')$, or column i of $\mathbf{G}^T(t - t')$, is the contribution at point i from all disturbance points j at time $t - t'$. Taking the partial derivative of $\mathbf{c}(t)$,

$$\frac{\partial\mathbf{c}(t)}{\partial\mathbf{q}(t')} = \mathbf{G}^T(t - t'), \tag{57}$$

consistent with the inference that the columns of the transpose of the Green function are the contributions (both relative and absolute) to the observed value at any point i to earlier disturbances at points j.

6. Transient Ages

[53] We return now to the problem of calculating age tracers as they evolve through time. Consider the $^3H/^3He$ parent-daughter product displayed in Figure 5 for which a Heaviside condition was imposed on the parent at $z = 0$, $t = 0$, with a decay constant λ appropriate for $^3H/^3He$ and $w > 0$ in the boundary layer regime. After about 150 years of calculation the apparent age is nearly asymptotic, but not completely so, at 800 m and above, with an age varying from 0 at the surface to about 60 years at 2000 m where it is still changing rapidly. Figure 5 also shows the identical calculation with λ chosen to be appropriate to ^{14}C. After 150 years the apparent age is still, unsurprisingly, changing rapidly and reaches from 0 at the surface to near 100 years at 2000 m. The two sets of apparent ages with depth after 159 model years are plotted together and are quantitatively different. As time increases, the patterns will eventually asymptote to the linear steady state of (43) with the very different final ages.

[54] The analytic Green function (31) can be applied to a perfect age tracer, with a steady interior source, resulting in

$$\begin{aligned}\tau(z,t) = \int_{t_0=0}^{t}\int_{z_0=-\infty}^{0}\frac{\sqrt{\kappa}}{2\sqrt{\pi(t-t_0)}}\exp\left[\frac{w(z-z_0)}{2\kappa}.-\frac{w^2(t-t_0)}{4\kappa}\right] \\ \cdot\left\{\exp\left[-\frac{(z-z_0)^2}{4\kappa(t-t_0)}\right]-\exp\left[-\frac{(z+z_0)^2}{4\kappa(t-t_0)}\right]\right\}dz_0dt_0,\end{aligned} \tag{58}$$

which is not very enlightening. If one could invert this expression for $t(z, \tau)$, it would be possible to associate a specific time with the perfect age tracer concentration as a function of z in a steady state; I

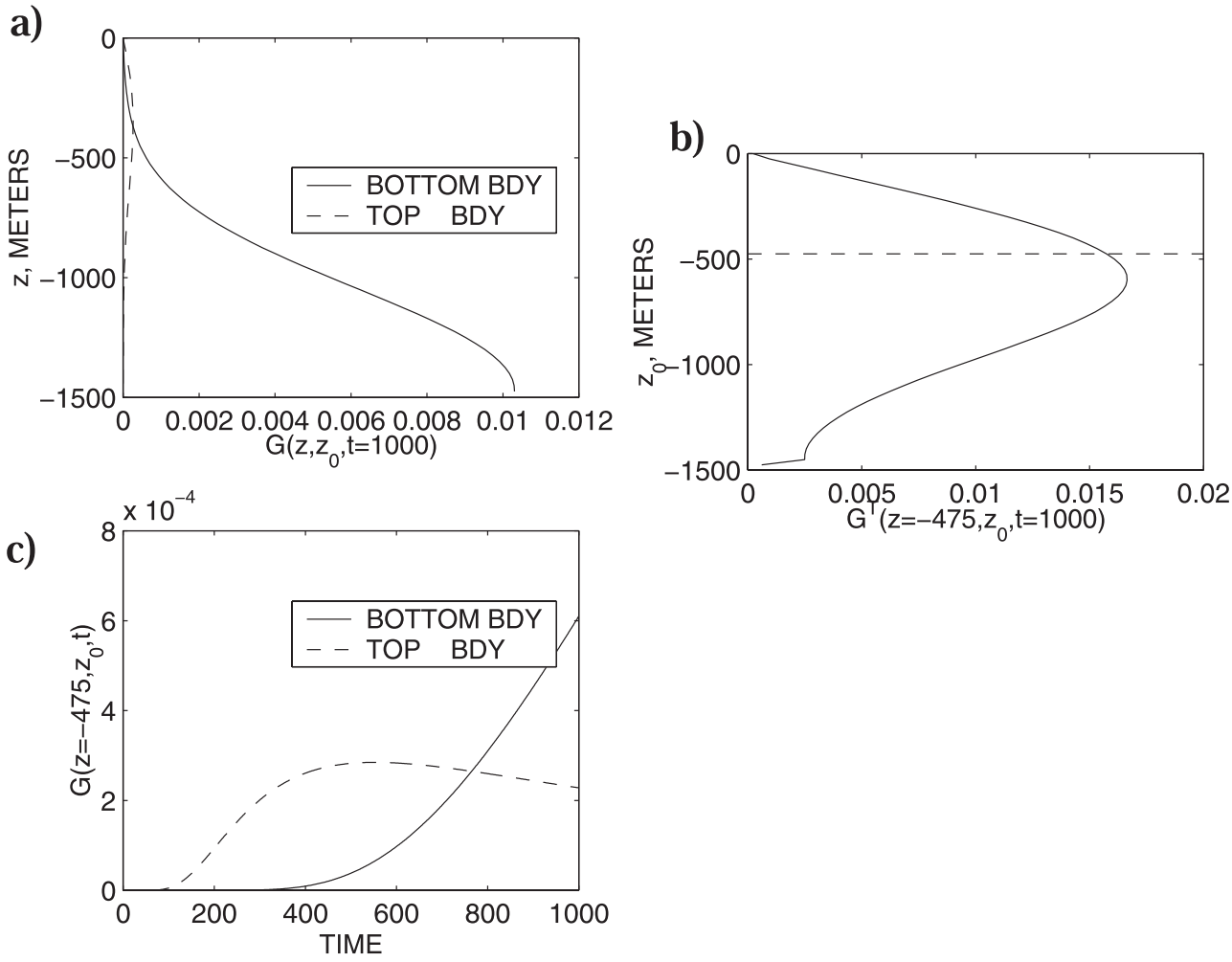

Figure 4. (a) Response computed numerically from (47) for sources at the top (dashed line) and bottom (solid line) after 1000 time steps. (b) The column of $\mathbf{G}^T$ corresponding to the concentration at $z = -475$ m (dashed line) at $t = 1000$, showing the sensitivity of the concentration at that depth to the concentration at all other depths at $t = 0$. If $t = 0$ concentrations are nonvanishing except at the top and bottom boundaries, the value at the bottom would dominate. (c) The time evolution of the contributions at 475 m depth from the two boundary points; evidently, by $t = 1000$ the contribution from the nearby surface value has peaked, and the concentration is dominated by water upwelling from the bottom as inferred from Figure 4b.

have not been able to find such an inversion, and it is probably not possible because the concentration at any time t is an integral over all past times. Similar expressions lead some investigators to the calculation of "probability density functions" for tracer present at a point.

7. Two-Dimensional Problems

[55] The one space dimension problem has proven intricate. Consider now the two-dimensional equation,

$$\frac{\partial C}{\partial t} + v\frac{\partial C}{\partial y} + w\frac{\partial C}{\partial z} - \kappa_z \frac{\partial^2 C}{\partial z^2} - \kappa_y \frac{\partial^2 C}{\partial y^2} = -\lambda C + q'_s(t,z), \quad (59)$$

which now involves u, and κ_y, with κ now denoted κ_z. For present purposes we will suppose that κ_z is interpreted as a diapycnal diffusivity and κ_y is an isopycnal value (or, mutatis mutandis, as dianeutral and epineutral values). Isopycnal and neutral surfaces, if used as the vertical coordinate, produce a non-Cartesian system, but as is usual, we neglect the resulting metric terms in the transformed advection/diffusion equation. The new parameters introduce at least three more timescales κ_y/u^2, L_y/u, and L_y^2/κ_y, where L_y is a basin width, with additional timescales possible from any temporal structure of a boundary condition on $y = 0$ and the interior flow. *Lee* [1999] has a brief discussion of analytic solutions in two dimensions, and others can be inferred from *Leij et al.* [1991]. We will omit displaying these and consider the purely numerical structure of the solutions. To focus the discussion, we will consider primarily the real age tracer problem.

[56] Equation (59) was discretized using a two-dimensional Dufort-Frankel leapfrog scheme, and as above, the statevector carries two time levels t, and $t - 1$. A number of physical situations are of interest. By way of illustration, Figure 6 was computed using $\kappa_z = 10^{-4}$ m^2 s^{-1}, $w = 10^{-7}$ m s^{-1}, $v = 10^{-2}$ m s^{-1}, $\kappa_y = 10^3$ m^2 s^{-1}, and $\lambda = 0$, with a concentration boundary condition $C(t, z = 0, y) = C_0H(t)$ at the surface and with zero concentration at $x = 0$. Although κ_z has been the subject of intense scrutiny in the literature, κ_y has been much less studied and is even more problematic, being difficult to distinguish from lateral geostrophic advection by flows on scales near the Rossby radius of deformation. *Ledwell et al.* [1998] suggest, on the basis of a purposeful tracer release experiment in the eastern North

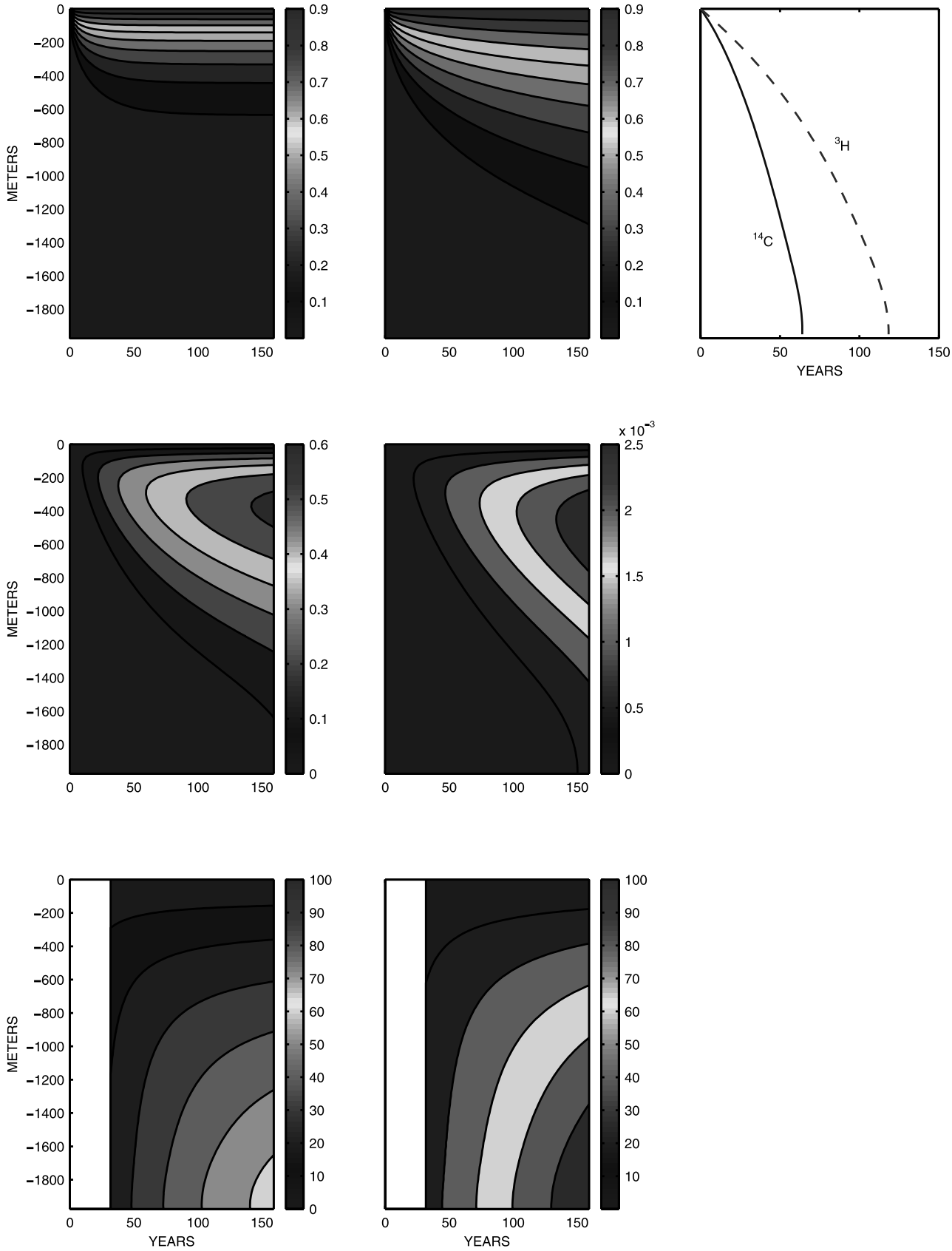

Figure 5. (left) The ^3H and ^3He distributions and (middle) $^{14}C/^{14}N$ through time for a Heaviside function surface source of the parent (^3H and ^{14}C, respectively) at $z = 0$. (right) The two differing age estimates after 159 years; they clearly depend upon the tracer being used. See color version of this figure at back of this issue.

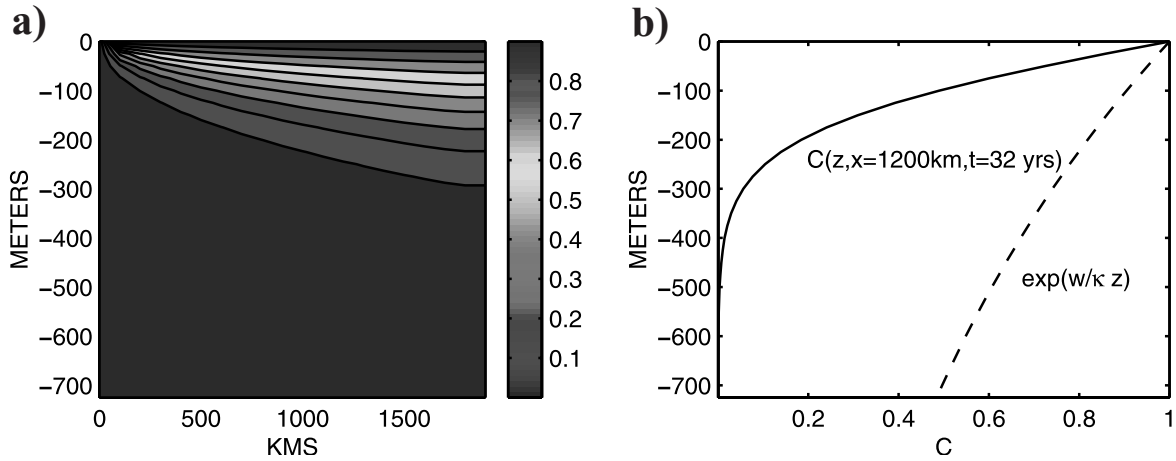

Figure 6. (a) Simple two-dimensional situation in which a Heaviside function nondecaying tracer was introduced at the sea surface but a flow from the left ventilates the fluid with zero concentration as well. (b) Comparison of the concentration profile at $x = 1200$ km with that arising from a pure one-dimensional advective-diffusive balance with the correct vertical parameters. See color version of this figure at back of this issue.

Atlantic, that large-scale behavior of their "patch" was consistent with values of $\kappa_y = 10^3$ m^2 s^{-1}, the value we have adopted.

[57] Conditions at the open boundaries were taken to be those of no diffusive flux [*Roache*, 1976]. With these parameters a steady state is reached quickly (within 30 years) with the result shown. Far from the boundary at $y = 0$, tracer distribution appears quite one dimensional and nearly exponential in shape (Figure 6b). If, however, one attempts to determine w/κ_z by a fit to this one-dimensional profile, the result is $\kappa_z/w \sim 200$ rather than the correct value of 1000. That is to say, the rapid ventilation from the north has carried low-concentration fluid into the central volume and confined the surface-injected tracer much closer to the sea surface than might be anticipated from a one-dimensional point of view. The inverse problem would have to be fully two-dimensional.

[58] We repeat the point that the concentration at any location is the result of integrating the Green function corresponding to all boundary points over all times $t' \leq t$; potentially, the value is dominated by the boundary condition at some particular location (surface or open boundary) at some particular time. That is evidently a very special case, and one that in any case, could only be demonstrated by carrying out the complete calculation. In three dimensions the problem is much compounded. Simple "thought experiments" attempting to make inferences about the circulation by comparison of tracer distributions having entered the ocean by different routes, boundary conditions, and timescales [e.g., *Broecker et al.*, 1999] are difficult to take seriously [see also *Orsi et al.*, 2001].

8. Stochastic Boundary Conditions

[59] A particularly interesting problem is that for which the tracer boundary condition is a space and/or time random variable, for example, in anomalies derived from surface evaporation/precipitation patterns. This subject is a very large one, raising numerous mathematical and practical issues, and is too much to pursue here. However, because the issues would necessarily arise in any use of observed tracers, which always have a stochastic element, some suggestive examples are summarized in Appendix B.

9. Summary and Conclusions

[60] What does all this add up to? Both the mathematical and physical behaviors of transient tracers are very interesting. The distribution of a tracer in the ocean at any time following its introduction at a boundary is an integral along the path (in space and time) of the tracer within the fluid ocean. Forward solutions at any given place and time are functions (equation (1)) of GCM flow, flow field mixing coefficients, and tracer model mixing, sources/sinks, and initial and boundary conditions as integrated over space and time. Thus the inverse problem is also a function of all these parameters and fields. Such a statement is almost generic, as it describes the behavior of all interesting oceanic observables, any of which is then a candidate for inference about the various parameters upon which the solutions depend. (Quantities such as velocity, pressure, or temperature are in principle simpler, however, as their description does not require the intervening tracer model in addition to the flow model.) As noted in section 1, the presence of a transient tracer, where zero tracer concentration existed previously, can be a dramatic and convincing demonstration of the existence of a fluid flow path or produce an order of magnitude estimate of transit ages and related quantities in ways that may be simpler than for other variables. One should not, however, overlook the possibility, for example, of obtaining equivalent timescales through the simple division of oceanic volumes by mass transport rates.

[61] Viewed in an inverse modeling context, the specific value of transient tracers for making quantitative inferences about the observed ocean circulation would depend directly upon the data distributions and the validity of various assumptions such as that of a steady state or impulsive boundary condition. An alternative statement is that one can clearly fit (i.e., solve the inverse problem, whether linear or nonlinear) any of the solutions here, either analytically or numerically, to the problem parameters and the associated initial and boundary conditions. The degree of skill, accuracy, and precision of the solution and its ease of attainment will depend directly upon the data itself and the accuracy of the model being used. From the resulting flow and diffusion variables all of the properties of the system could then be calculated, including any plausible age definition. One can do similar fits with steady state tracers or velocity or other observed fields, and whether a particular data type is especially effective cannot be decided in the abstract.

[62] As the various solutions depicted here show, the behavior of a transient tracer even in a one-dimensional steady situation is an intricate function of numerous timescales and space scales deriving from geometry, tracer decay, and boundary conditions, further complicated by any space scales (and timescales) belonging to

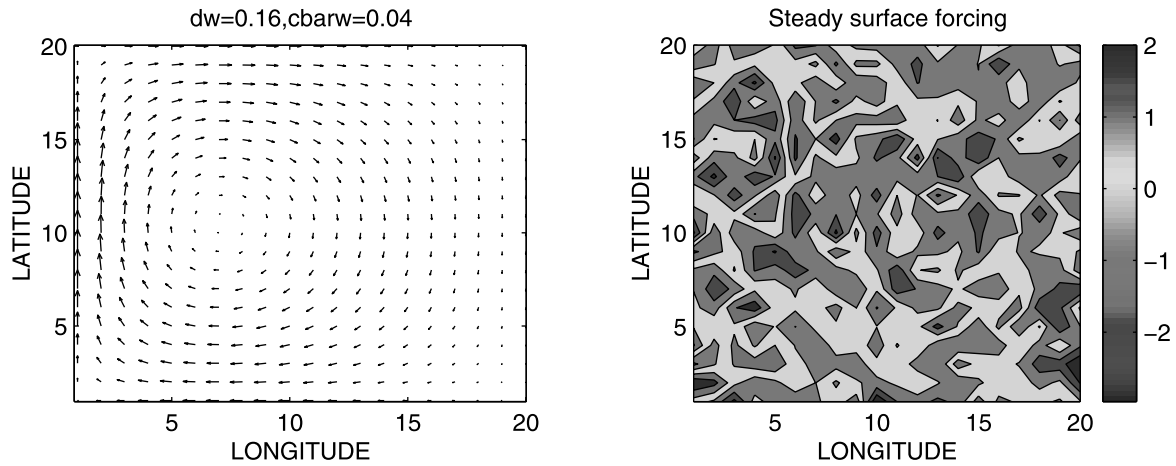

Figure B1. (left) A steady Stommel gyre and (right) a steady, but random (spatial white noise), tracer boundary condition imposed on the flow. See color version of this figure at back of this issue.

the flow field. With adequate data all fluid and tracer parameters can be inferred. Whether the transient tracers carry more information about κ, and **u** relative to the distribution of a steady state tracer cannot be answered in general; it depends upon the distribution of the available data and the extent to which other potentially uncertain parameters such as $C_B(t)$ are known. Of course, for the steady state problem one must also be concerned about errors in the steady boundary conditions.

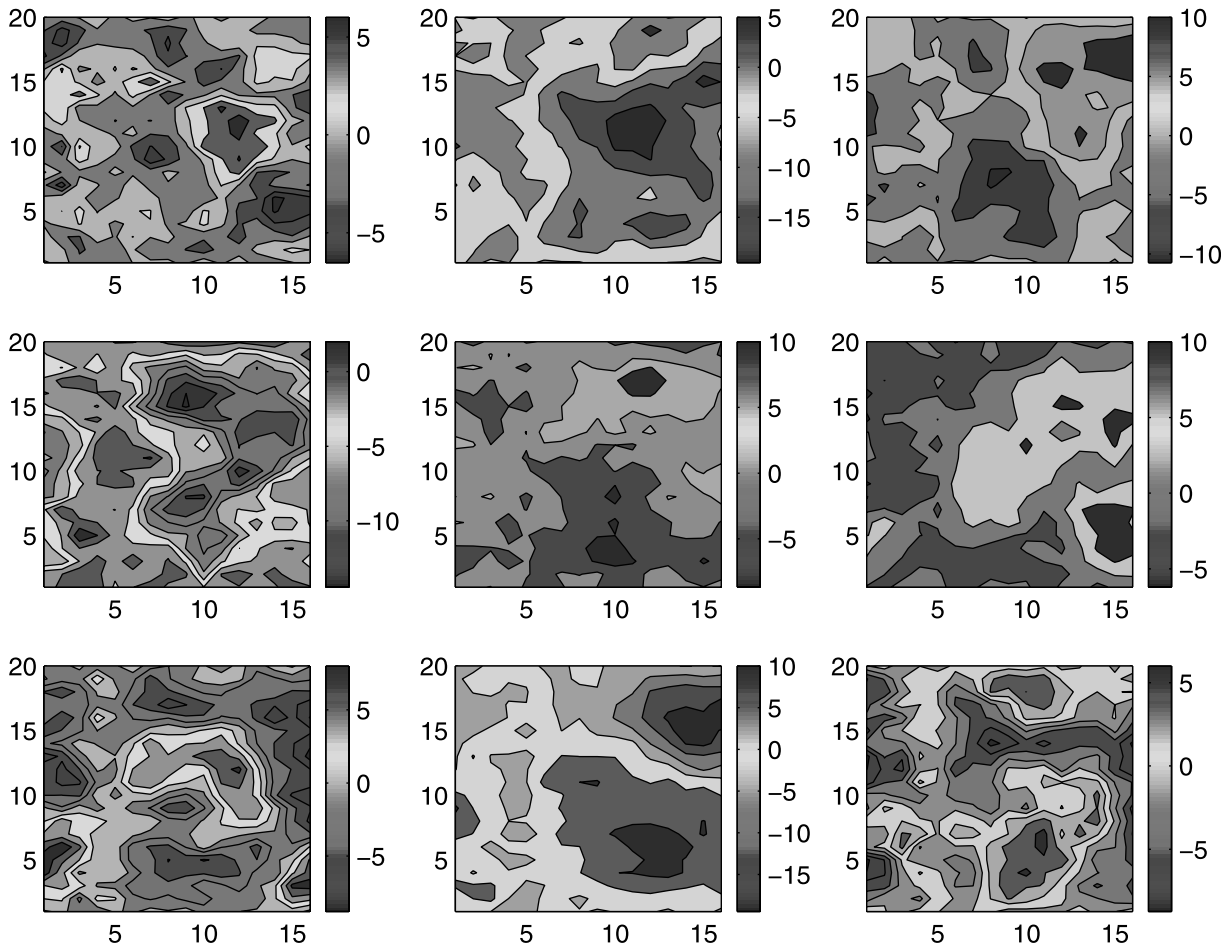

Figure B2. Nine separate steady tracer distributions all resulting from different steady but spatially white noise tracer boundary condition as in the single example in Figure B1. All structures present are larger in scale than anything in the boundary conditions and are the result of the flow and diffusion; the underlying flow field is difficult to discern. See color version of this figure at back of this issue.

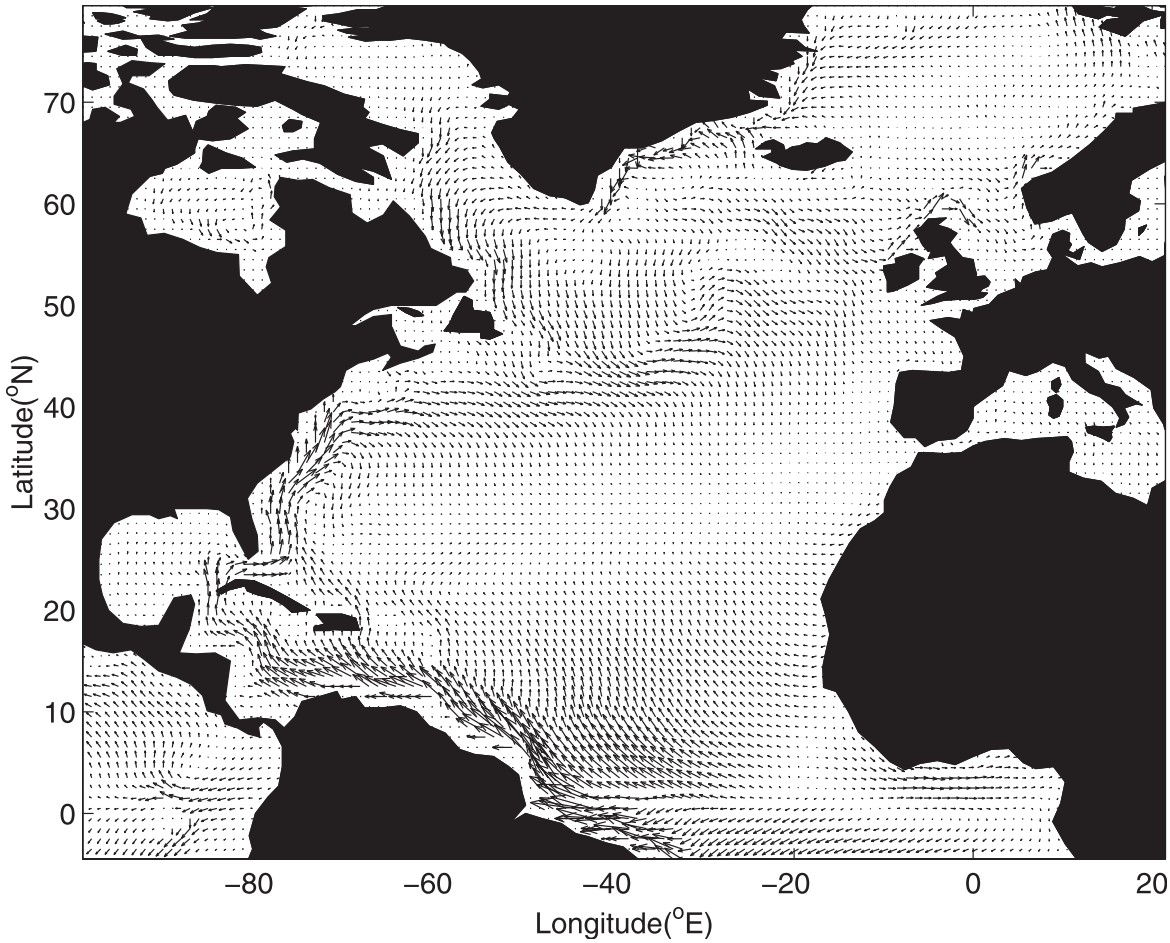

Figure B3. Average (1985–1997) February surface flow from the general circulation model used to study behavior of stochastic surface boundary conditions [*Marshall et al.*, 1997]. Model time step was 3 hours. Maximum flow arrow is 0.7 m s^{-1}.

[63] Age tracers that are derived from the more basic observable ones remain functions of these identical parameters, albeit the functional forms are more complex. For an inverse problem directed at estimating some combination of κ, $\mathbf{u}$, and $C_B(t)$, little or nothing appears to be gained by using a derived age tracer, and something may well be lost. There are applications [e.g., *Gruber et al.*, 1996] where one seeks a time since a fluid parcel was at the sea surface so as to set, for example, a bomb radiocarbon boundary condition. The $^3H/^3He$- or CFC-derived age is supposed to produce a useful number. As we have seen, however, in any two-dimensional or higher problem the properties found at any location $\mathbf{r}$ are an integral over all possible boundary data at boundary positions $\mathbf{r}_B$ from earlier times. If one has the boundary Green function $\mathbf{G}(\mathbf{r}, \mathbf{r}_B, t, t')$ at a particular time t, the sensitivity to the surface condition at $\mathbf{r}_B$ at time $t' < t$ is known. To calculate the concentration of some tracer at $\mathbf{r}_B$, and t, one must integrate the Green function for that tracer; there is no shortcut and no single time. It is the Green function that is fundamental; everything else is a computable consequence.

[64] Many of the concerns expressed here about the use of tracers with observations become moot when their primary use is the theoretical application to diagnostics of a GCM. There one can make very specific assumptions about tracer behavior, essentially defining the governing equation, and use it as a diagnostic description of what the model does to that hypothetical tracer (see, e.g., the discussion by *Delhez et al.* [1999]; even in models, the situation is not simple). To some degree it is a matter of taste whether one best tests a model by comparing its tracer distribution to one that is observed or whether one infers, for example, κ from the data and compares it to the model value.

Appendix A: Continuous Time and Discrete Space

[65] The partial discretization with time left continuous has a number of uses, and we here record the resulting formalism. Following *Wunsch* [1987], (7) is discretized with a centered-in-space scheme as

$$\frac{\partial C_i}{\partial t} = C_{i-1}\left[\frac{wT}{2\Delta z} + \frac{\kappa T}{(\Delta z)^2}\right] + C_i\left[-\lambda T - \frac{2\kappa T}{(\Delta z)^2}\right] + C_{i+1}\left[-\frac{wT}{2\Delta z} + \frac{\kappa T}{(\Delta z)^2}\right] + Tq_{si}$$
$$= C_{i-1}\left[\frac{\bar{c}}{2} + d\right] + C_i[l - 2d] + C_{i+1}\left[-\frac{\bar{c}}{2} + d\right] + q'_{si}. \quad \text{(A1)}$$

Here T is the dimensional timescale, and $\bar{c} = wT/\Delta z = \kappa/(w\Delta z)$, $d = \kappa T/(\Delta z)^2 = \kappa^2/(w\Delta z)^2$, and $l = \lambda T = \lambda\kappa/w^2$ are dimensionless parameters.

[66] With time as a continuous variable, we can exploit the slightly tidier notation for solutions of differential equations as

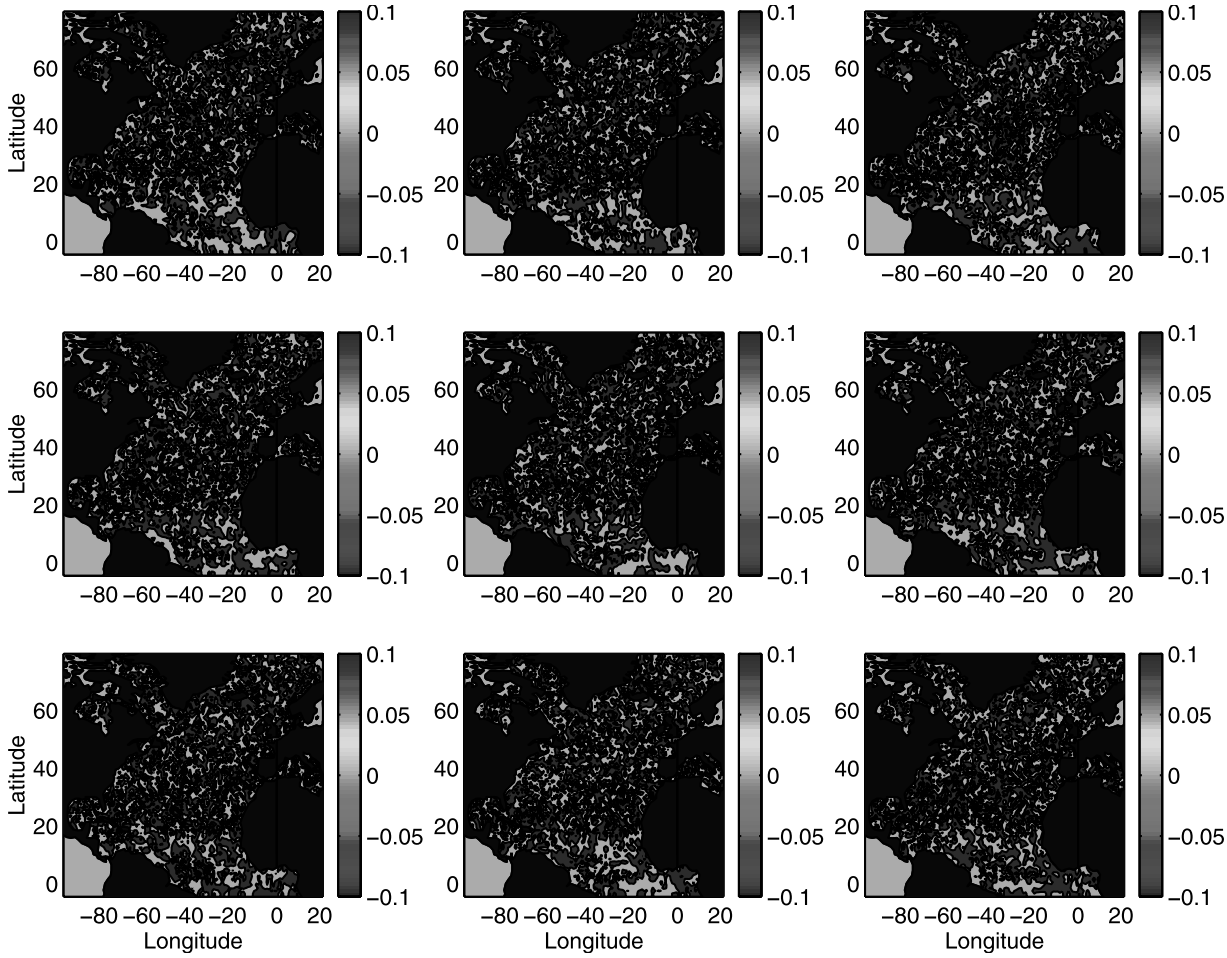

Figure B4. White noise (both space and time) surface tracer boundary conditions applied to the off-line model corresponding to the GCM flow in Figure B3. Actual distributions present at the beginning of successive years are shown, but the distributions were held fixed for 1 month before being changed. See color version of this figure at back of this issue.

opposed to those of difference equations. Equation (A1) can be written in canonical form for the vector of unknowns as

$$\frac{\partial \mathbf{c}(t)}{\partial t} = \mathbf{A}\mathbf{c}(t) + \mathbf{q}_s', \quad \mathbf{c}(t) = [C_i(t)], \tag{A2}$$

where the state transition matrix is

$$\mathbf{A} = \begin{Bmatrix} 0 & 0 & 0 & \dots & 0 & 0 & 0 \\ \gamma & \alpha & \beta & \dots & 0 & 0 & 0 \\ 0 & \gamma & \alpha & \beta & 0 & \dots & 0 \\ 0 & 0 & \dots & 0 & \gamma & \alpha & \beta \\ 0 & 0 & \dots & 0 & 0 & 0 & 0 \end{Bmatrix} \tag{A3}$$

with

$$\gamma = \frac{\bar{c}}{2} + d, \alpha = l - 2d, \ \beta = -\frac{\bar{c}}{2} + d. \tag{A4}$$

The first and last grid point values are fixed by boundary conditions (here imposed through q'_s). $\mathbf{A}$ is independent of time for steady w. The general solution to (A2) is [e.g., *Bellman*, 1960]

$$\mathbf{c}_m(t) = e^{\mathbf{A}t}\mathbf{c}_m(0) + \int_0^t e^{\mathbf{A}(t-t')}\mathbf{q}'_s(t')dt', \tag{A5}$$

where $\mathbf{c}_m(0)$ are the initial conditions.

[67] A time-dependent flow can be discretized in space with time left continuous. A periodic flow, representing, for example, the seasonal cycle would be a special case. Unfortunately, the resulting simple system with a periodic state transition matrix $\mathbf{A}$ is, as stated by *Bellman* [1960, p. 201], one of "extreme difficulty." One might hope to use one of the Green functions displayed above by, for example, invoking a very slow oscillation time, but the large values of the timescales T_i show that the annual cycle, as one example, is much too short to be treated as quasi-steady.

[68] In spatial finite difference form the coupled tracer equations are then

$$\frac{\partial \mathbf{c}_1(t)}{\partial t} = \mathbf{A}_1 c_1(t) + \mathbf{q}_s'(t), \quad \mathbf{c}_1(t) = [C_{1i}(t)], \tag{A6}$$

$$\frac{\partial \mathbf{c}_2(t)}{\partial t} = \mathbf{A}_2\mathbf{c}_2(t) + \lambda\mathbf{c}_1(t), \quad \mathbf{c}_2(t) = [C_{2i}(t)], \tag{A7}$$

where $\mathbf{A}_1 = \mathbf{A}$, as in (A3); $\mathbf{A}_2$ is the same as $\mathbf{A}$, except with $\lambda = 0$. The growth of ^{3}He does not affect the time evolution of ^{3}H, so that the solution to (A6) is simply

$$\mathbf{c}_1(t) = \int_0^t e^{\mathbf{A}_1(t-t')}\mathbf{q}'_{1s}(t')dt' \tag{A8}$$

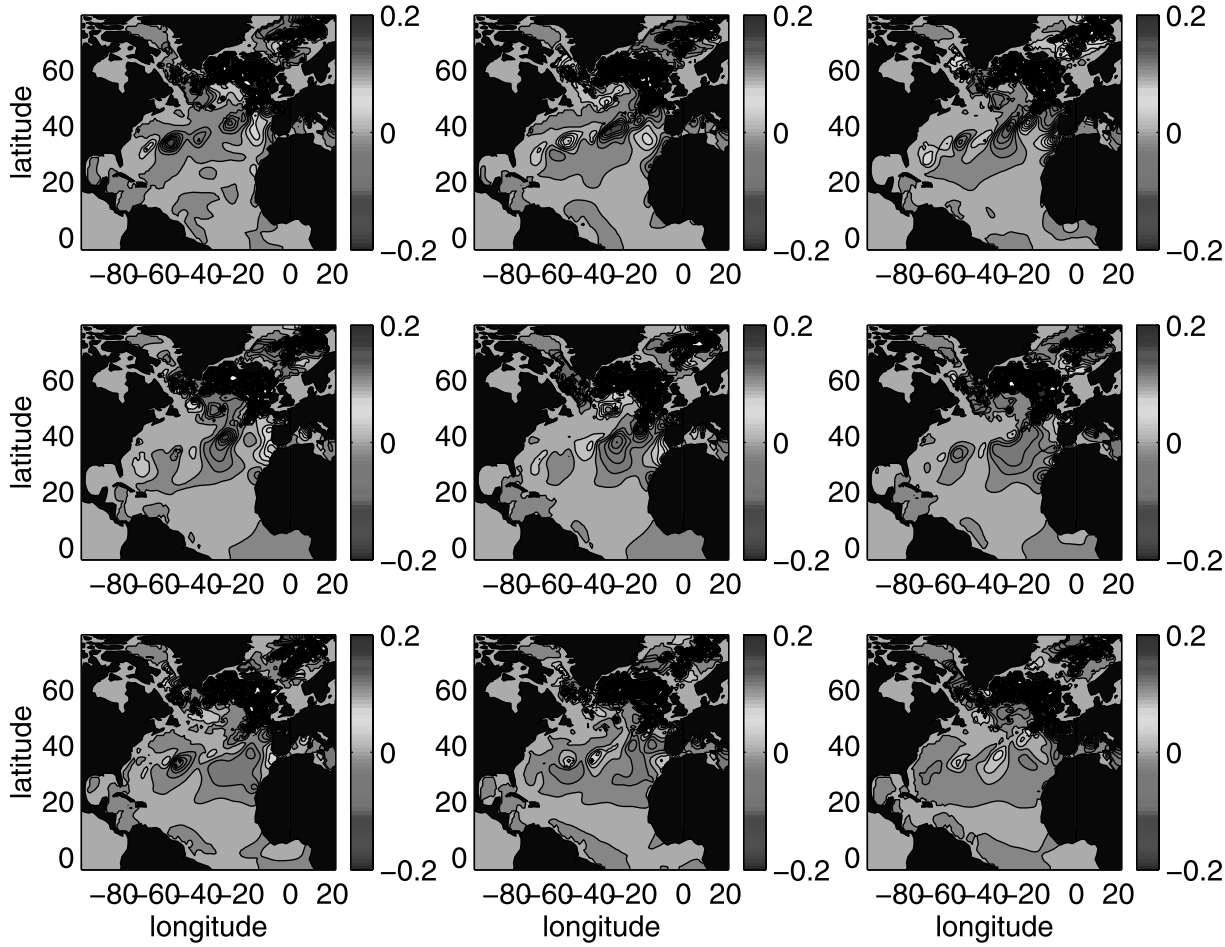

Figure B5. Tracer concentration at 510 m at yearly intervals from white noise surface boundary conditions. There is a large-scale time-evolving pattern wholly a consequence of the model flow and unconnected to any structure in the boundary conditions. See color version of this figure at back of this issue.

using an initial condition of $\mathbf{c}_1(t) = 0$, which is approximately valid for ^{3}H prior to about 1950. The solution to (A7) is then

$$\mathbf{c}_2(t) = \lambda \int_0^t e^{\mathbf{A}_2(t-t'')} \mathbf{c}_1(t'')dt'' = \lambda \int_0^t e^{\mathbf{A}_2(t-t'')} \left[\int_0^{t''} e^{\mathbf{A}_1(t''-t')} \mathbf{q}'_{1s}(t')dt' \right] dt''. \quad \text{(A9)}$$

This form makes fully explicit the nature of the solution as an integral over the full time and space history of the parent or underlying forcing. A somewhat tidier form can be obtained by defining

$$\mathbf{c}_3 = \begin{bmatrix} \mathbf{c}_1 \\ \mathbf{c}_2 \end{bmatrix}, \mathbf{A}_3 = \begin{Bmatrix} \mathbf{A}_1 & \mathbf{0} \\ \lambda\mathbf{I} & \mathbf{A}_2 \end{Bmatrix}, \mathbf{q}'_3(t) = \begin{bmatrix} \mathbf{q}'_{1s}(t) \\ \mathbf{0} \end{bmatrix} \quad \text{(A10)}$$

and then

$$\mathbf{c}_3(t) = \mathbf{A}_3\mathbf{c}_3(t) + \mathbf{q}'_3(t), \quad \text{(A11)}$$

which is the same type as (A2) and hence with the same solution form as well. The control literature [e.g., *Brogan*, 1985] has a broad discussion of methods for accurate discrete representation of the canonical form (A2). These numerical expressions reproduce well the analytical solutions described in the text.

Appendix B: Stochastic Forcing

[69] The numerical methodology lends itself to the study of the situation in which the tracer forcing is stochastic, rather than being the deterministic transients so-far considered. There seems little doubt that much of the observed climate variability is best understood as a random walk of a series of coupled systems (atmosphere/ocean/cryosphere/...); exactly what fractions of observed structures on any timescale are primarily stochastic rather than deterministic remains uncertain. Even on shorter timescales than climatic ones, tracer boundary conditions inevitably contain a random component, both from fluctuations in air/sea transfers and from observational noise.

[70] An interesting example is to regard the evaporation/precipitation forcing of the sea surface by the atmosphere as generating a random tracer, the salinity anomaly, at the sea surface. These anomalies will then evolve under the physics of the surface circulation, assuming the anomaly is sufficiently weak not to disturb the circulation and that there is no feedback to the atmosphere. Of particular interest is the question of whether such phenomena as the so-called "Great Salinity Anomaly" [*Dickson et al.*, 1988] can be regarded as the expected fluctuations in a random walk behavior [e.g., *Wunsch*, 1992] or whether they must be regarded as the result of a deterministic change in the climate

system. These questions are related to the theory of stochastic climate change [*Hasselmann*, 1976].

[71] As a simple example, consider a Stommel gyre (Figure B1) governing the flow field in (59) but with $\kappa_z = \kappa_x$. Suppose the tracer source, $q(x, y)$ is a purely white noise process in space (see Figure B1) but is still held steady in time. Then the system will ultimately reach a steady state governed by

$$\mathbf{c}_\infty = \mathbf{A}\mathbf{c}_\infty + \mathbf{q}. \tag{B1}$$

The final tracer distribution to which the system evolves in time is thus

$$\mathbf{c}_\infty = (\mathbf{I} - \mathbf{A})^{-1}\mathbf{q}. \tag{B2}$$

Figure B2 shows examples of nine different asymptotic tracer fields corresponding to nine different random fields **q**. The tracer fields contain large scales, most of which are not obviously connected with any structure in the forcing field (recall, it is spatially white noise), and neither is it apparent, to the eye at least, what the underlying flow field is. Here the inverse problem would require knowledge of **q** and some insight into the number of parameters governing the flow field (i.e., the number of independent parameters determining matrix **A**). The inverse problem would then be set as the determination of those parameters [see, e.g., *Wunsch*, 1985].

[72] The Stommel gyre is very simple. What happens if one attempts to use a time-varying, more realistic flow? Figure B3 is the average surface flow over 1 month from the Massachusetts Institute of Technology model [*Marshall et al.*, 1997], which was integrated over the period 1985–1997. A white (in both space and time) surface anomaly was imposed at each time step, again to be thought of as possibly a freshwater anomaly of sufficiently small magnitude that to first order it does not have dynamical consequences. Under these circumstances the only structures that can emerge in the tracer field are those imposed by the flow field itself. Instantaneous results at yearly intervals are shown at 510 m in Figures B4 and B5. A similar but weaker pattern appears at greater depths (not shown; I am indebted to X. Li for these results). Large-scale patterns do emerge at depth, with an intriguing structure that waxes and wanes unpredictably over the time of integration.

[73] A full understanding of how these patterns develop, what their timescales and space scales are, and how they vary in the vertical requires the analysis tools of stochastic differential equations, a large and well-developed subject [e.g., *Gardiner*, 1990] far beyond our present scope. Evidently, however, there is much to be learned.

[74] **Acknowledgments.** I thank T. Haine, A. Plumb, and the anonymous referees for useful comments. I was supported in part by the National Ocean Partnership Program (NOPP) through the ECCO Consortium with funding from the U.S. National Science Foundation, the National Aeronautics and Space Administration, and the Office of Naval Research.

References

Bellman, R., *Introduction to Matrix Analysis*, McGraw-Hill, New York, 1960. (reprinted by Soc. for Ind. and Appl. Math., Philadelphia, Pa., 1995.)

Boudreau, B. P., *Diagentic Models and Their Implementation: Modelling Transport and Reactions in Aquatic Sediments*, Springer-Verlag, New York, 1997.

Broecker, W. S., and T. H. Peng, *Tracers in the Sea*, 690 pp., Lamont-Doherty Earth Obs., Palisades, N. Y., 1982.

Broecker, W. S., S. Sutherland, and T. H. Peng, A possible 20th-century slowdown of Southern Ocean deep water formation, *Science*, *286*, 1132–1135, 1999.

Brogan, W. L., *Modern Control Theory*, 2nd ed., 393 pp., Prentice-Hall, Old Tappan, N. J., 1985.

Butkovskiy, A. G., *Green's Functions and Transfer Functions Handbook*, 236 pp., Ellis Horwood, Chichester, U. K., 1982.

Carslaw, H. S., and J. C. Jaeger, *Conduction of Heat in Solids*, 2nd ed., 510 pp., Clarendon, Oxford, U. K., 1986.

Craig, A. P., J. L. Bullister, D. E. Harrison, R. M. Chervin, and A. M. Semtner Jr., A comparison of temperature, salinity and chlorofluorocarbon observations with results from a 1° resolution three dimensional ocean model, *J. Geophys. Res.*, *103*, 1099–1119, 1998.

Delhez, E. J. M., J.-M. Campin, A. C. Hirst, and E. Deleersnijder, Toward a general theory of the age in ocean modelling, *Ocean Modelling*, *1*, 17–28, 1999.

Dickson, R. R., J. Meincke, S.-A. Malmberg, and A. Jake, The great salinity anomaly, *Prog. Oceanogr.*, *20*, 103–151, 1988.

Doney, S. C., W. J. Jenkins, and J. L. Bullister, A comparison of ocean tracer dating techniques on a meridional section in the eastern North Atlantic, *Deep Sea Res., Part I*, *44*, 603–626, 1997.

Duffy, P. B., E. E. Eliason, A. J. Bourgeois, and C. C. Covey, Simulation of bomb radiocarbon in two global ocean general circulation models, *J. Geophys. Res.*, *100*, 22,545–22,563, 1995.

England, M. H., and E. Maier-Reimer, Using chemical tracers to assess ocean models, *Rev. Geophys.*, *39*, 29–70, 2001.

England, M. H., V. Garçon, and J.-F. Minster, Chlorofluorocarbon uptake in in a world ocean model, 1, Sensitivity to the surface gas forcing, *J. Geophys. Res.*, *99*, 25,215–25,233, 1994.

Gardiner, C. W., *Handbook of Stochastic Methods for Physics, Chemistry and the Natural Sciences*, 2nd ed., Springer-Verlag, New York, 1990.

Gray, S. L., and T. W. N. Haine, Constraining a North Atlantic Ocean general circulation model with chlorofluorocarbon observations, *J. Phys. Oceanogr.*, *31*, 1157–1181, 2001.

Gruber, N., J. L. Sarmiento, and T. F. Stocker, An improved method for detecting anthropogenic CO_2 in the ocean, *Global Biogeochem. Cycles*, *10*, 809–837, 1996.

Hall, T. M., and R. A. Plumb, Age as a diagnostic of stratospheric transport, *J. Geophys. Res.*, *99*, 1059–1070, 1994.

Hasselmann, K., Stochastic climate models, part 1, Theory, *Tellus*, *28*, 473–485, 1976.

Hirst, A. C., Determination of water component age in ocean models: Application to the fate of North Atlantic Deep Water, *Ocean Modell. 1*, pp. 81–94, Hooke Inst., Oxford, U. K., 1999.

Holzer, M., and T. M. Hall, Transt-time and tracer-age distributions in geophysical flows, *J. Atmos. Sci.*, *57*, 3539–3558, 2000.

Jenkins, W. J., 3-H and 3-He in the beta triangle: Observations of gyre ventilation and oxygen utilization rates, *J. Phys. Oceanogr.*, *17*, 763–783, 1987.

Jenkins, W. J., The use of anthropogenic tritium and helium-3 to study subtropical gyre ventilation and circulation, *Philos. Trans. R. Soc., London, Ser. A*, *325*, 43–61, 1988.

Kay, A., Advection-diffusion in reversing and oscillating flows, II, Flows with multiple reversals, *IMA J. Appl. Math.*, *58*, 185–210, 1997.

Kelley, D. E., and K. A. van Scoy, A basinwide estimate of vertical mixing in the upper pycnocline: Spreading of bomb tritium in the North Pacific Ocean, *J. Phys. Oceanogr.*, *29*, 1759–1771, 1999.

Khatiwala, S., M. Visbeck, and P. Schlosser, Age trancers in an ocean GCM, *Deep Sea Res., Part I*, *48*, 1423–1441, 2001.

Ledwell, J. R., A. J. Watson, and C. S. Law, Mixing of a tracer in the pycnocline, *J. Geophys. Res.*, *103*, 21,499–21,529, 1998.

Lee, T.-C., *Applied Mathematics in Hydrogeology*, 382 pp., A. F. Lewis, New York, 1999.

Leij, F. J., T. H. Skagos, and M. T. van Genuchten, Analytical solutions for solute transport in three-dimensional semi-infinite porous media, *Water Resources Res.*, *27*, 2719–2733, 1991.

Marshall, J., A. Adcroft, C. Hill, L. Perelman, and Heisey, A finite-volume, incompressible Navier Stokes model for studies of the ocean on parallel computers, *J. Geophys. Res.*, *102*, 5753–5766, 1997.

Mémery, L., and C. Wunsch, Constraining the North Atlantic circulation with ^{3}H data, *J. Geophys. Res.*, *95*, 5229–5256, 1990.

Menemenlis, D., and C. Wunsch, Linearization of an oceanic general circulation model for data assimilation and climate studies, *J. Atmos. Oceanic Technol.*, *14*, 1420–1443, 1997.

Monin, A. S., and A. M. Yaglom, *Statistical Fluid Mechanics: Mechanics of Turbulence*, 874 pp., MIT Press, Cambridge, Mass., 1975.

Moore, W. S., R. M. Key, and J. L. Sarmiento, Techniques for precise mapping of ^{226}Ra and ^{238}Ra in the ocean, *J. Geophys. Res.*, *90*, 6983–6994, 1985.

Morse, P. M., and H. Feshbach, *Methods of Theoretical Physics*, 1978 pp., McGraw-Hill, New York, 1953.

Munk, W., Abyssal recipes, *Deep Sea Res.*, *13*, 707–730, 1966.

Munk, W., and C. Wunsch, Abyssal recipes, II, Energetics of tidal and wind mixing, *Deep Sea Res.*, *45*, 1976–2009, 1998.

Nauman, E. B., and B. A. Buffham, *Mixing in Continuous Flow Systems*, 271 pp., Wiley-Interscience, New York, 1983.

Neu, J. L., and R. A. Plumb, Age of air in a "leaky pipe" model of stratospheric transport, *J. Geophys. Res.*, *104*, 19,243–19,255, 1999.

Orsi, A. H., S. S. Jacobs, A. L. Gordon, and M. Visbeck, Cooling and ventilating the abyssal ocean, *Geophys. Res. Lett.*, *28*, 2923–2926, 2001.

Ottino, J. M., *The Kinematics of Mixing: Stretching, Chaos, and Transport*, 364 pp., Cambridge Univ. Press, New York, 1989.

Reddy, S. C., and L. N. Trefethen, Pseudospectra of the convection-diffusion operator, *SIAM J. Appl. Math.*, *54*, 1634–1649, 1994.

Roache, P. J., *Computational Fluid Dynamics*, 446 pp., Hermosa, Albuquerque, N. M., 1976.

Robbins, P. E., and W. J. Jenkins, Observations of temporal changes of tritium-helium-3 age in the eastern North Atlantic thermocline: Evidence for changes in ventilation, *J. Mar. Res.*, *56*, 1125–1161, 1998.

Shraiman, B. I., and E. D. Siggia, Scalar turbulence, *Nature*, *405*, 639–646, 2000.

Stammer, D., and C. Wunsch, The determination of the large-scale circulation of the Pacific Ocean from satellite altimetry using model Green's functions, *J. Geophys. Res.*, *101*, 18,409–18,432, 1996.

Wahrhaft, Z., Passive scalars in turbulent flows, *Annu. Rev. Fluid Mech.*, *32*, 203–240, 2000.

Weiss, R. F., J. L. Bullister, R. H. Gammon, and M. J. Warner, Atmospheric chlorofluoromethanes in the deep equatorial Atlantic, *Nature*, *314*, 608–610, 1985.

Wunsch, C., Can a tracer field be inverted for velocity?, *J. Phys. Oceanogr.*, *15*, 1521–1531, 1985.

Wunsch, C., Using transient tracers: The regularization problem, *Tellus, Ser. B*, *39*, 477–492, 1987.

Wunsch, C., Eclectic modelling of the North Atlantic, II, Transient tracers and the ventilation of the eastern basin thermocline, *Philos. Trans. R. Soc., Ser. A*, *325*, 201–236, 1988.

Wunsch, C., Decade-to-century changes in the ocean circulation, *Oceanography*, *5*, 99–106, 1992.

Wunsch, C., *The Ocean Circulation Inverse Problem*, 437 pp., Cambridge Univ. Press, New York, 1996.

Yamanaka, G., Y. Kitamura, and M. Endoh, Formation of North Pacific Intermediate Water in Meteorological Research Institute ocean general circulation model, 2, Transient tracer experiments, *J. Geophys. Res.*, *103*, 30,905–30,921, 1998.

C. Wunsch, Program in Atmospheres, Oceans and Climate, Department of Earth, Atmospheric and Planetary Sciences, Massachusetts Institute of Technology, Cambridge, MA 02139, USA. (cwunsch@mit.edu)

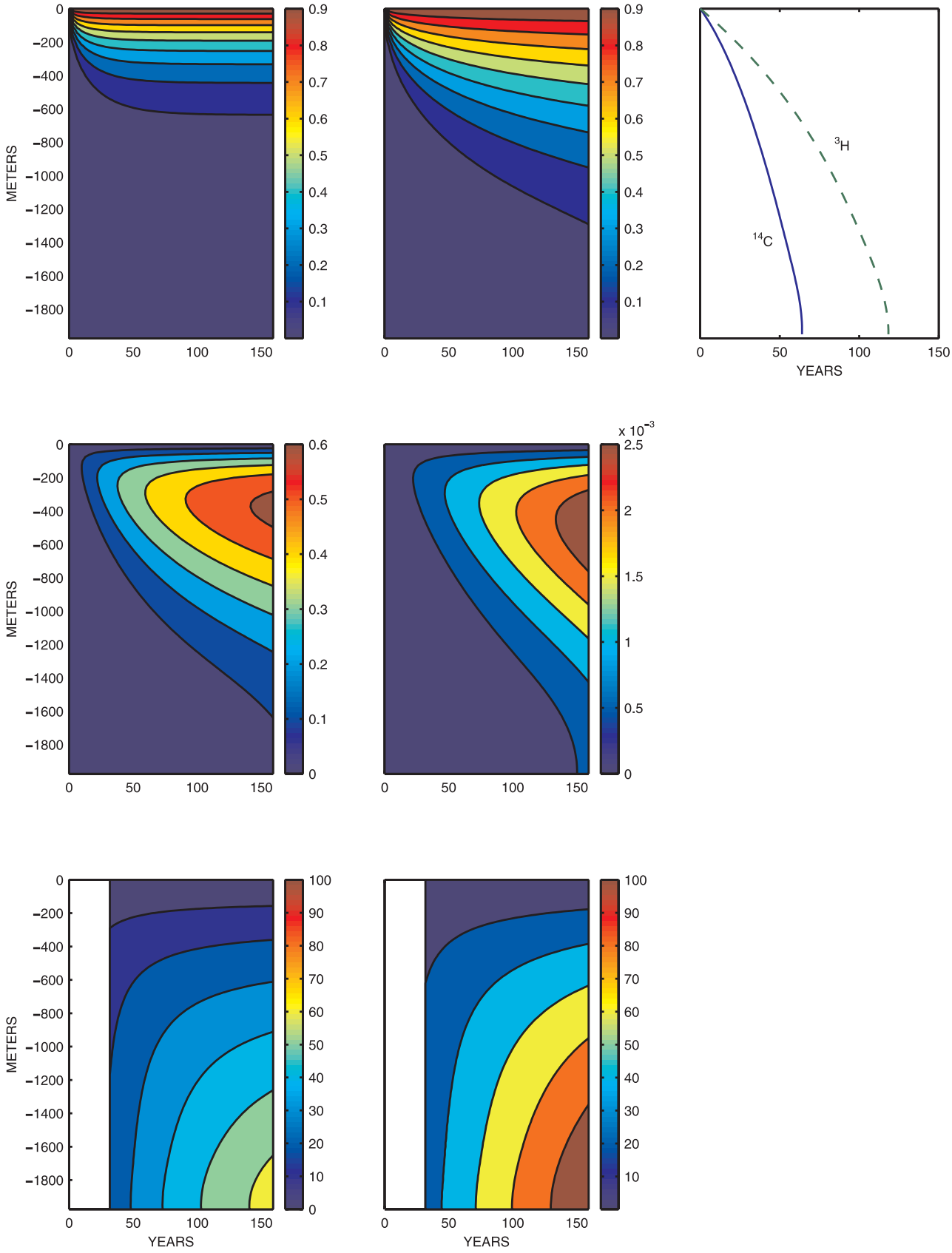

Figure 5. (left) The ^{3}H and ^{3}He distributions and (middle) $^{14}C/^{14}N$ through time for a Heaviside function surface source of the parent (^{3}H and ^{14}C, respectively) at $z = 0$. (right) The two differing age estimates after 159 years; they clearly depend upon the tracer being used.

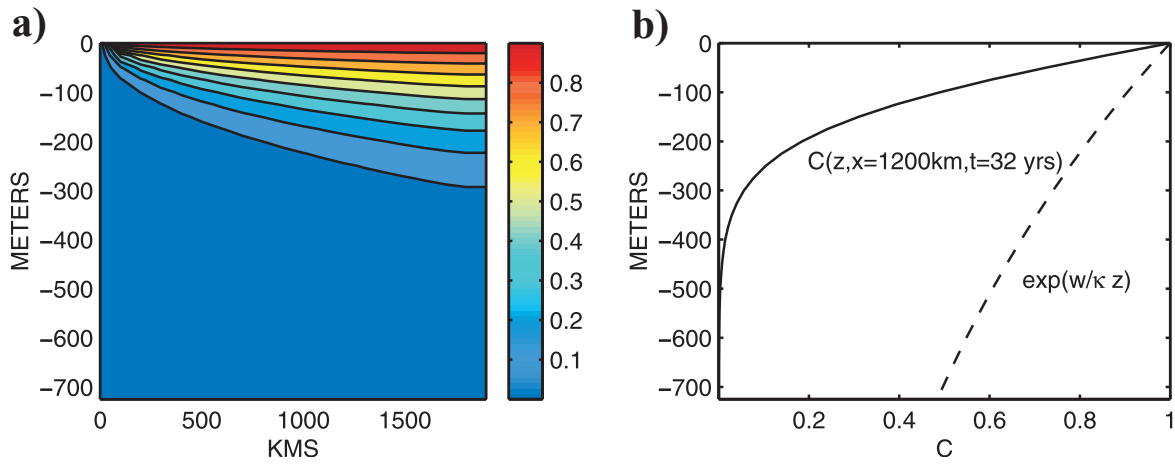

Figure 6. (a) Simple two-dimensional situation in which a Heaviside function nondecaying tracer was introduced at the sea surface but a flow from the left ventilates the fluid with zero concentration as well. (b) Comparison of the concentration profile at x = 1200 km with that arising from a pure one-dimensional advective-diffusive balance with the correct vertical parameters.

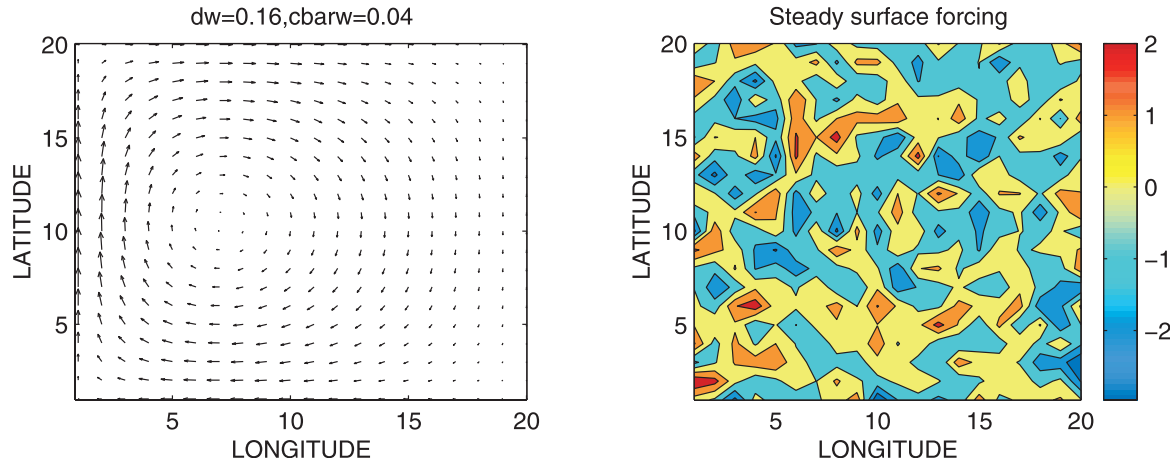

Figure B1. (left) A steady Stommel gyre and (right) a steady, but random (spatial white noise), tracer boundary condition imposed on the flow.

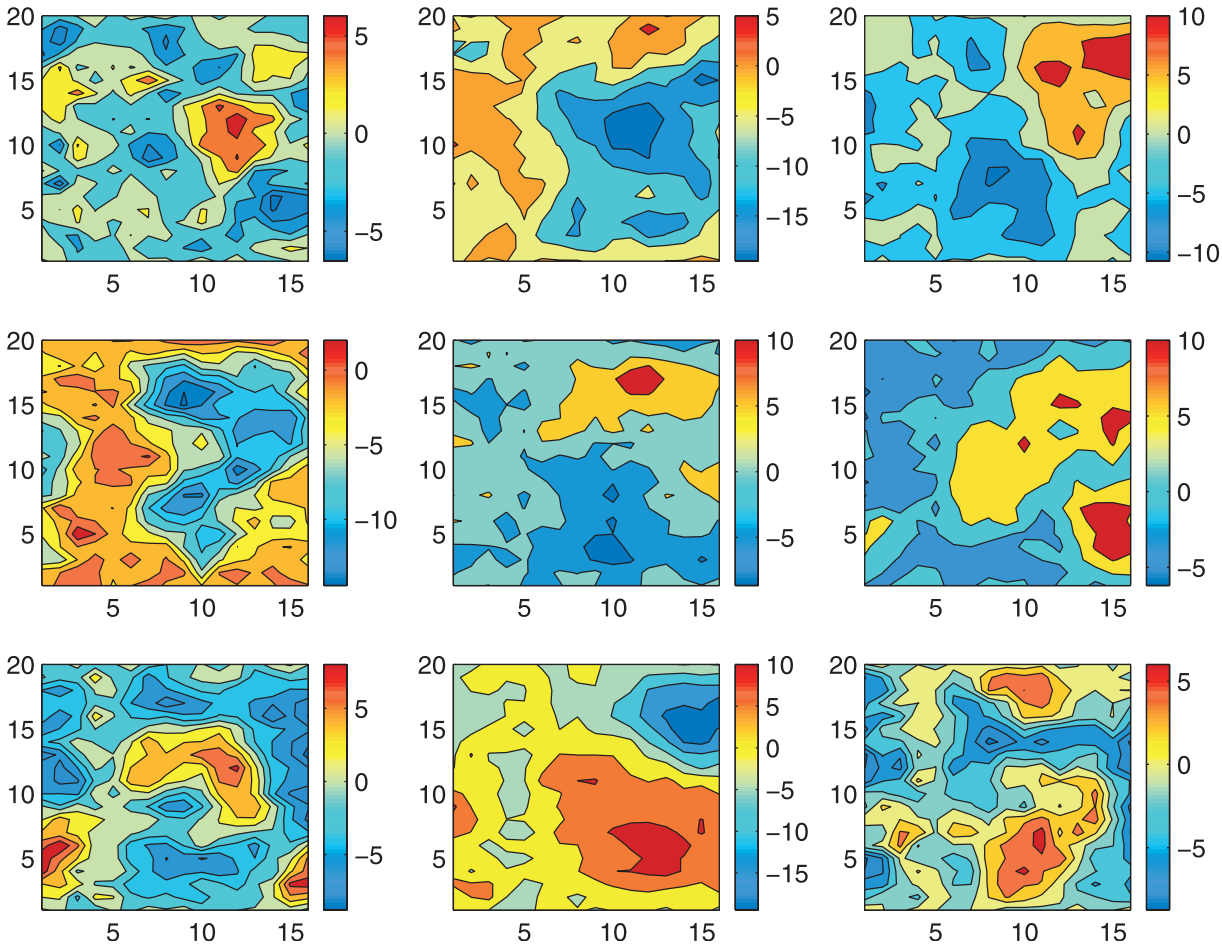

Figure B2. Nine separate steady tracer distributions all resulting from different steady but spatially white noise tracer boundary condition as in the single example in Figure B1. All structures present are larger in scale than anything in the boundary conditions and are the result of the flow and diffusion; the underlying flow field is difficult to discern.

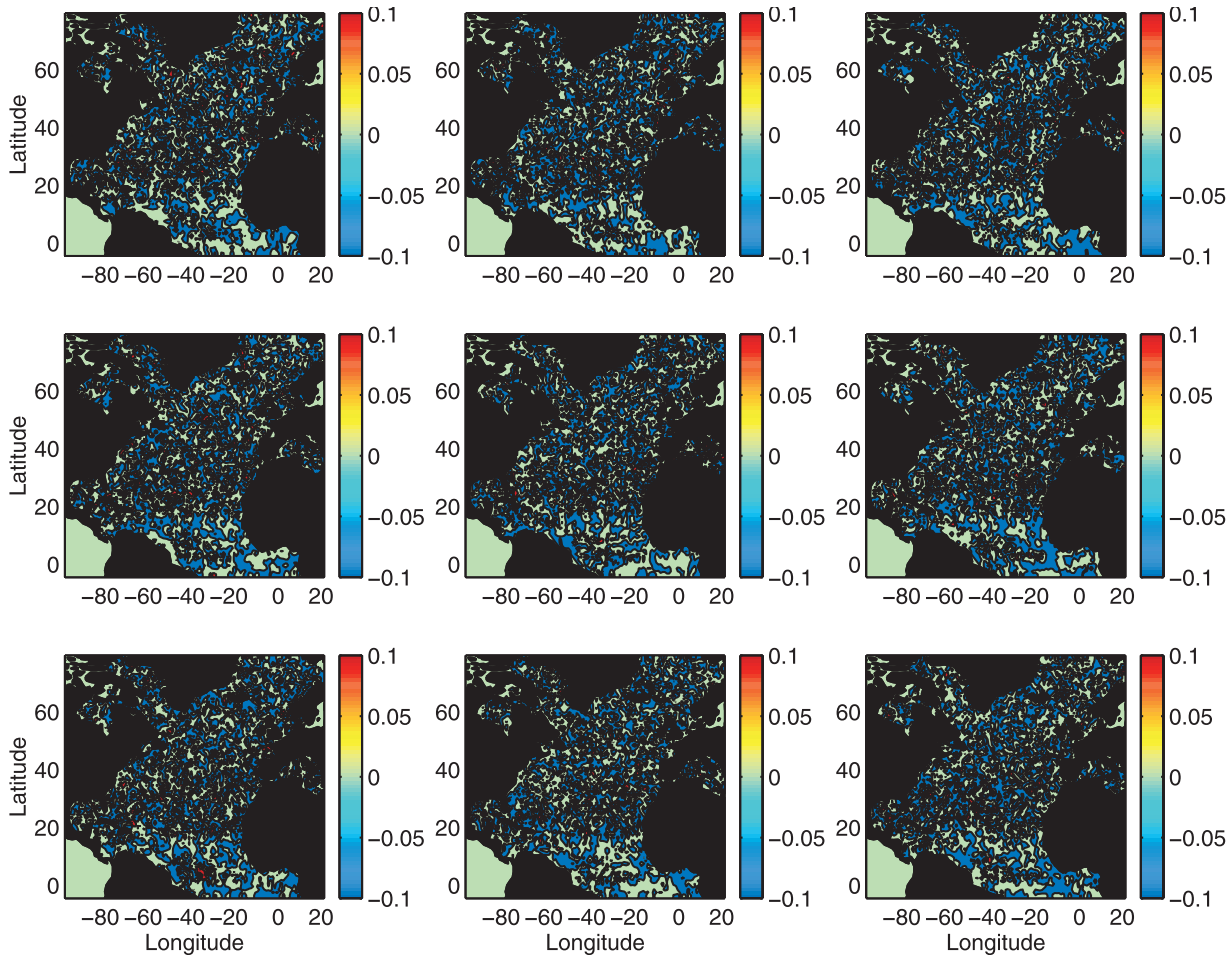

Figure B4. White noise (both space and time) surface tracer boundary conditions applied to the off-line model corresponding to the GCM flow in Figure B3. Actual distributions present at the beginning of successive years are shown, but the distributions were held fixed for 1 month before being changed.

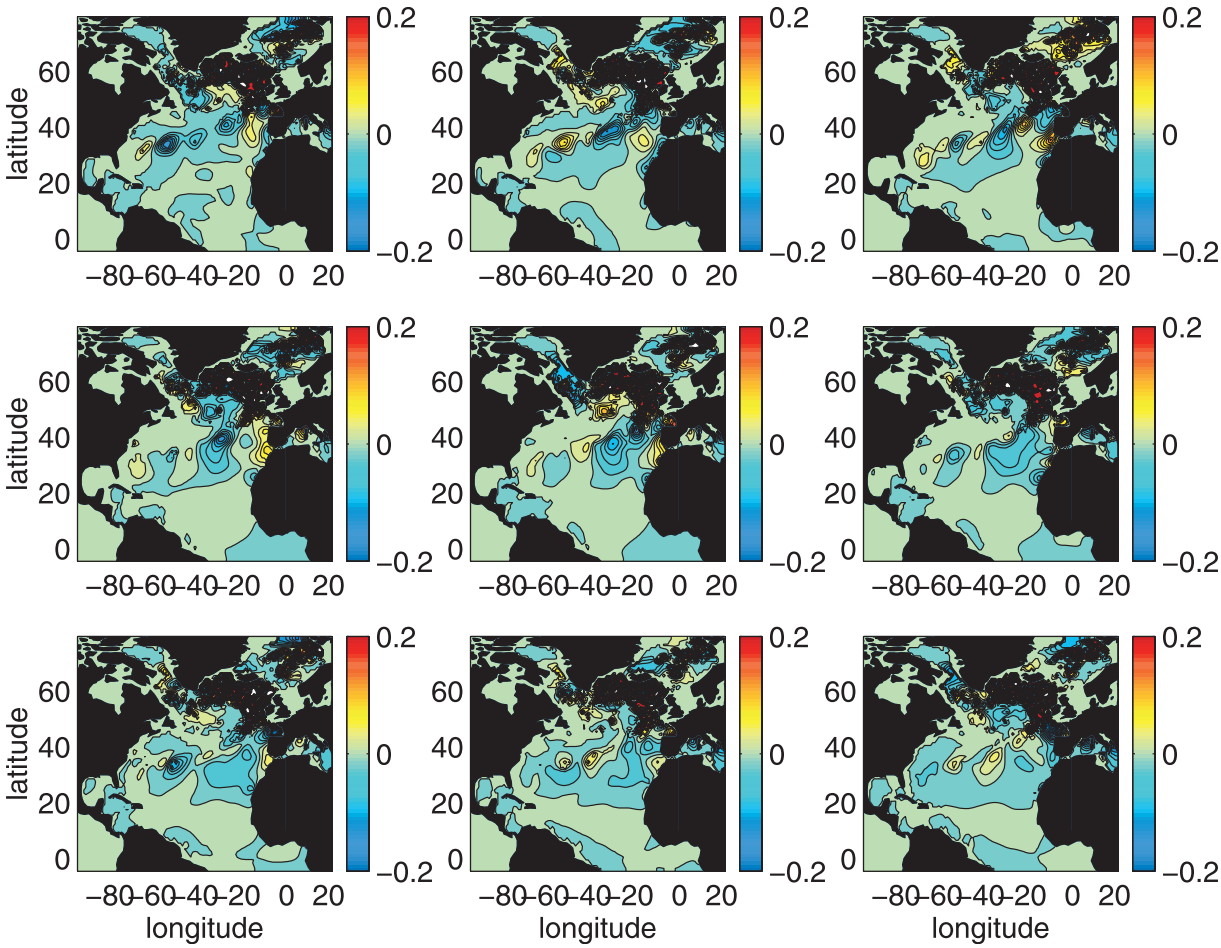

Figure B5. Tracer concentration at 510 m at yearly intervals from white noise surface boundary conditions. There is a large-scale time-evolving pattern wholly a consequence of the model flow and unconnected to any structure in the boundary conditions.